Synthesis and anticancer activity of 2,4-disubstituted furo[3,2-b] indole derivatives

ARTICLE *in* EUROPEAN JOURNAL OF MEDICINAL CHEMISTRY · JUNE 2013

Impact Factor: 3.45 · DOI: 10.1016/j.ejmech.2013.06.012 · Source: PubMed

9 AUTHORS, INCLUDING:

Weiting Liu
National Cheng Kung University
156 PUBLICATIONS **3,435** CITATIONS
SEE PROFILE

Hsu Mei Hua
21 PUBLICATIONS **270** CITATIONS
SEE PROFILE

European Journal of Medicinal Chemistry 66 (2013) 466–479

Contents lists available at SciVerse ScienceDirect

European Journal of Medicinal Chemistry

journal homepage: http://www.elsevier.com/locate/ejmech

Original article

Synthesis and anticancer activity of 2,4-disubstituted furo[3,2-*b*]indole derivatives

Shi-Hong Zhuang [a], Yi-Chien Lin [a], Li-Chen Chou [a], Mei-Hua Hsu [a], Hui-Yi Lin [a], Chi-Hung Huang [b], Jin-Cherng Lien [a], Sheng-Chu Kuo [a], Li-Jiau Huang [a,*]

[a] *Graduate Institute of Pharmaceutical Chemistry, China Medical University, No. 91 Hsueh-Shih Road, Taichung 40402, Taiwan ROC*
[b] *Taiwan Advance Biopharm, Inc., 12F, No. 25, Lane 169, Kangning Street, Xizhi District, New Taipei City 221, Taiwan, ROC*

ARTICLE INFO

Article history:
Received 8 February 2013
Received in revised form
23 May 2013
Accepted 7 June 2013
Available online 18 June 2013

Keywords:
Furo[3,2-*b*]indole derivatives
Structure–activity relationships (SARs)
Anticancer activity
A498 renal cancer cells

ABSTRACT

We synthesized and evaluated a series of 2,4-disubstituted furo[3,2-*b*]indole derivatives for anticancer activity and established the structure–activity relationships (SARs) of these compounds. Among all tested compounds, we found (5-((2-(hydroxymethyl)-4*H*-furo[3,2-*b*]indol-4-yl)methyl)furan-2-yl) methanol (**10a**) to be the most promising agent. In screening against NCI-60 human tumor cell lines, **10a** exhibited highly selective anticancer activity and significant inhibitory activity against A498 renal cancer cells. Our COMPARE analysis results suggest that the **10a** fingerprint is similar to that of NSC-754549, which is an isostere of **YC-1**. We further confirmed the significant antitumor activity of compound **10a** with tests in the A498 xenograft nude mice model. Therefore, compound **10a** should be further developed as a new drug candidate for treating renal cancer.

1. Introduction

The 1-benzyl-3-(5-hydroxymethyl-2-furyl)indazole (YC-1) is a highly potent anticancer drug candidate with multiple biological activities, including anti-angiogenesis [1,2], anti-inflammation [3], and apoptosis induction [4,5] activities as well as the ability to inhibit matrix metalloproteinases (MMPs) [6]. Studies on YC-1 in various antitumor animal models, such as non-small cell lung cancer [2], renal cancer [7], and breast cancer [8], have all confirmed its significant anticancer activity.

The core skeleton of YC-1 is an indazole. We previously applied the concept of bioisosterism to replace the indazole ring of YC-1 with furo[3,2-*c*]pyrazole (A) [9], thieno[3,2-*c*]pyrazole (B) [10], and selenolo[3,2-*c*]pyrazole (C) [11] in an effort to discover YC-1 analogs with potential anticancer activity. We also synthesized a series of these analogs with different core skeletons and evaluated their anticancer activity to establish the structure–activity relationships (SARs) of YC-1 analogs (Chart 1).

Our findings showed that all A-, B-, and C-type compounds exhibited similar SARs, and those with 3-furanylcarbinol and 1-methylaryl moieties demonstrated significant and selective anticancer activity. Although the exact role of these two moieties is unclear, from a molecular biology viewpoint, we continued modifying the structure of YC-1 analogs, by fusing its furan ring with the indole ring to form a new core structure consisting of expanded tricyclic furo[3,2-*b*]indole (D). By adding a fourth type of YC-1 analogs with a novel core structure, we attempted to establish enhanced SARs, leading to the development of a more profound anticancer drug candidate. We separately introduced similar functional groups used previously, namely, the CH_2OH-bearing group and the CH_2–Ar group, onto the 2-position and 4-position of the new skeleton. We synthesized and evaluated the analogs of this new core skeleton for anticancer activity.

2. Results and discussion

2.1. Chemistry

Scheme 1 schematically shows the synthetic routes to the target compounds (**1**–**3**, **6a**–**c**, **7a**–**o** and **10a**–**c**). Starting compound **1** [12] was reacted with various alkyl halides (**4a**, **4b**), substituted benzyl halides (**4c**–**o**), and heteroarylmethyl halides (**8a**–**c**) [13] in the presence of NaH to yield the corresponding methyl 4-substituted furo[3,2-*b*]indole-2-carboxylates (**5**, **9**). The ester compounds **5a**–**o** and **9a**–**c** were either hydrolyzed with 10% NaOH to the corresponding carboxylic acids (**3**, **6a**–**c**) or reduced with Ca

* Corresponding author. Tel.: +886 4 22053366x5609; fax: +886 4 22030760.
E-mail address: ljhuang@mail.cmu.edu.tw (L.-J. Huang).

0223-5234/$ – see front matter © 2013 Elsevier Masson SAS. All rights reserved.
http://dx.doi.org/10.1016/j.ejmech.2013.06.012

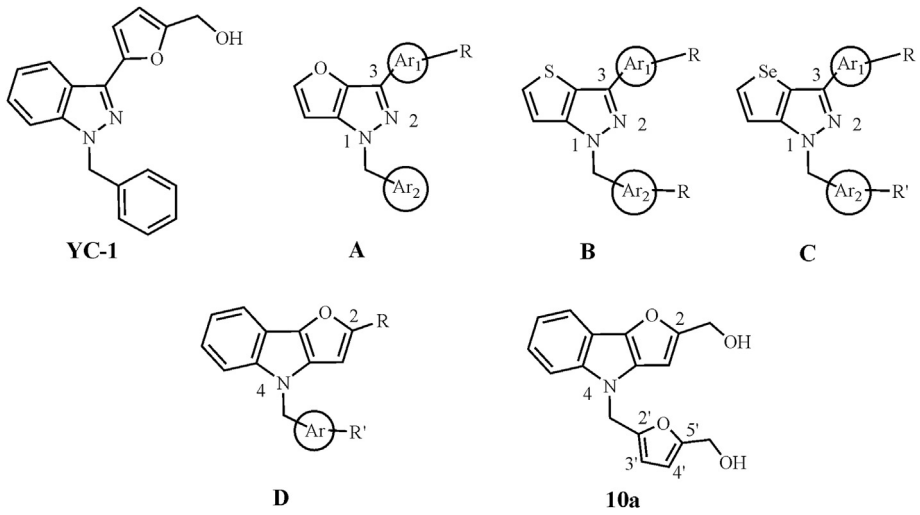

Chart 1. Structures of YC-1 analogs.

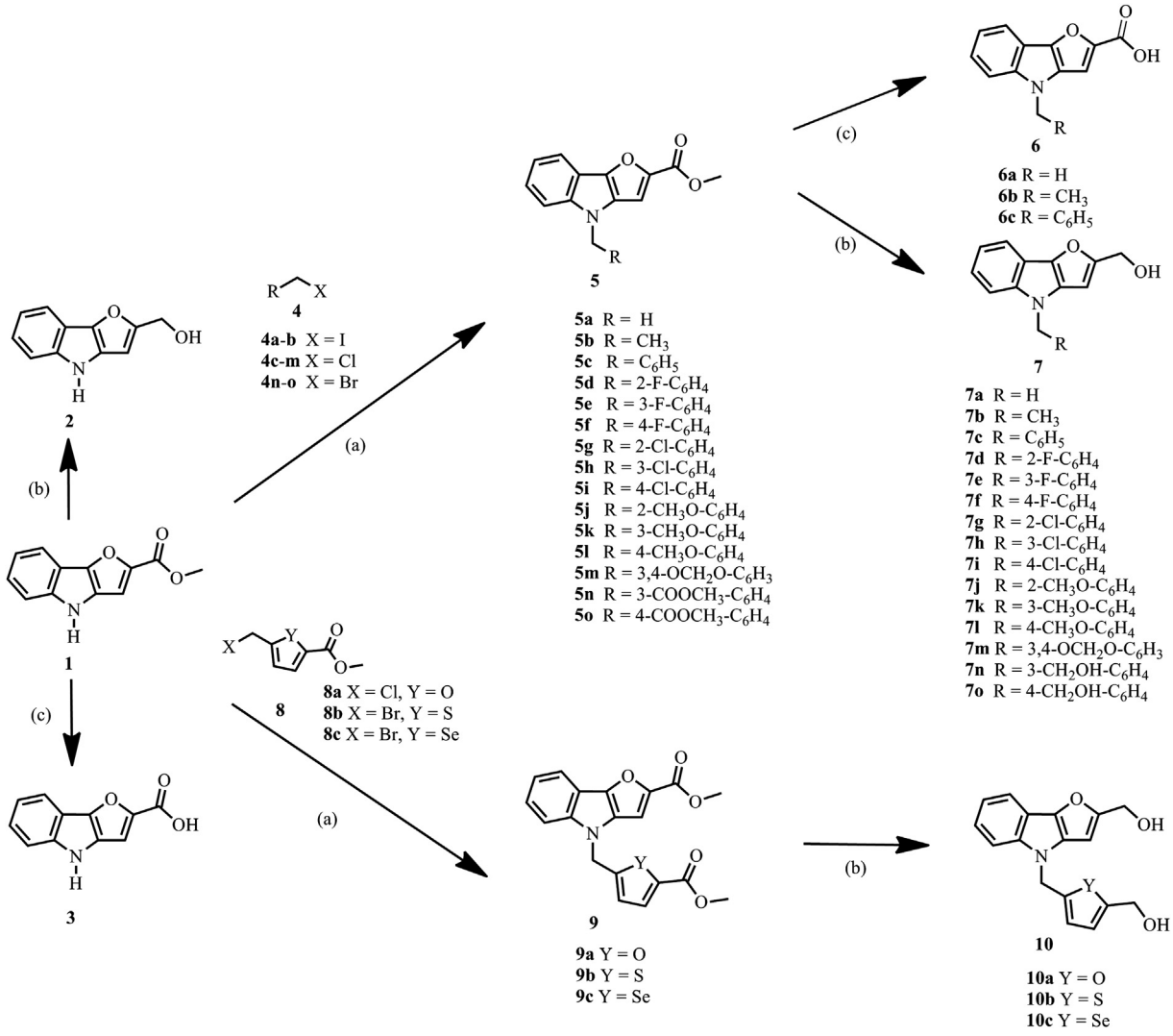

Scheme 1. Reagents and conditions: (a) NaH/DMF; (b) $Ca(BH_4)_2$/THF; (c) (1) 10% NaOH (2) dilute HCl.

$(BH_4)_2$ to afford the corresponding carbinols **7a**–**o** and **10a**–**c**. The chemical structures of the target compounds were determined based on their HRMS and NMR spectra.

2.2. Screening tests of compounds *1–3, 5a–o, 6a–c, 7a–o, 9a–c and 10a–c*

We evaluated the newly synthesized target compounds (**1**–**3**, **5a**–**o**, **6a**–**c**, **7a**–**o**, **9a**–**c** and **10a**–**c**) for growth–inhibitory activity against five human cancer cell lines: HL-60 leukemia, Hep 3B hepatoma, H460 non-small cell lung cancer, A498 renal cancer, and COLO 205 colon cancer lines. We simultaneously tested Detroit 551 normal human fetal skin fibroblast cells with the target compounds for comparison. The results are summarized in Table 1. Compound **2** exhibited the greatest inhibitory activity among compounds **1**–**3** against the A498 renal cancer cell line (IC_{50} = 21.8 μM). Replacement of the CH_2OH group (R_2) of compound **2** with a $COOCH_3$ group (**1**) or with a COOH group (**3**) resulted in reduced inhibitory activity against the A498 cell line (IC_{50} > 50 μM). In contrast, replacement of the H (R_4) of compound **2** with a CH_3 group (**7a**), a C_2H_5 group (**7b**), or a benzyl group (**7c**) increased inhibitory activity against the A498 cell line in the order of compound **2** (R_4 = H, IC_{50} = 21.8 μM) < **7a** (R_4 = CH_3, IC_{50} = 4.6 μM) < **7b** (R_4 = C_2H_5, IC_{50} = 3.7 μM) < **7c** (R_4 = benzyl, IC_{50} = 0.24 μM). Larger substituents at R_4 improved inhibitory activity against the A498 renal cancer cell line, which improved by as much as 100-fold over compound **2**. Among the five cell lines tested, these compounds showed selective inhibitory activity against the A498 renal cancer

Table 1
Cytotoxicity of compounds **1**–**3**, **5a**–**o**, **6a**–**c**, **7a**–**o**, **9a**–**c** and **10a**–**c**.

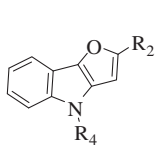

(1-3, 5a-b, 6a-b, 7a-b)

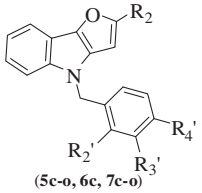

(5c-o, 6c, 7c-o)

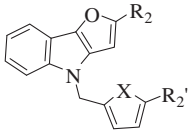

(9a-c, 10a-c)

Compd no.	X	R_2	R_4	$R_{2'}$	$R_{3'}$	$R_{4'}$	IC_{50} (μM)[a]					
							HL-60	Hep 3B	H460	A498	COLO 205	Detroit 551
1	–	$COOCH_3$	H	–	–	–	>50	>50	>50	>50	>50	>50
2	–	CH_2OH	H	–	–	–	>50	>50	>50	21.8	>50	>50
3	–	COOH	H	–	–	–	>50	>50	>50	>50	>50	>50
5a	–	$COOCH_3$	CH_3	–	–	–	>50*	>50*	50	>50*	>50*	>50*
5b	–	$COOCH_3$	C_2H_5	–	–	–	>50	>50	>50	>50	>50	>50
5c	–	$COOCH_3$	–	H	H	H	>50*	>50*	>50*	>50*	>50*	>50*
5d	–	$COOCH_3$	–	F	H	H	>50*	>50*	>50*	>50*	>50*	>50*
5e	–	$COOCH_3$	–	H	F	H	>50*	>50*	>50*	>50*	>50*	>50*
5f	–	$COOCH_3$	–	H	H	F	>50*	>50*	>50*	>50*	>50*	>50*
5g	–	$COOCH_3$	–	Cl	H	H	>50*	>50*	>50*	>50*	>25	>50*
5h	–	$COOCH_3$	–	H	Cl	H	>50*	>50*	>50*	>50*	>50*	>50*
5i	–	$COOCH_3$	–	H	H	Cl	>50*	>50*	>50*	>50*	>50*	>50*
5j	–	$COOCH_3$	–	OCH_3	H	H	25.1	50*	>50*	>50*	32.9	>50
5k	–	$COOCH_3$	–	H	OCH_3	H	>50	>50	>50	>50	>50	>50
5l	–	$COOCH_3$	–	H	H	OCH_3	>50	58.6	>50	>50	>50	>50
5m	–	$COOCH_3$	–	H	$-OCH_2O-$		>50	>50	>50	>50	>50	>50
5n	–	$COOCH_3$	–	H	$COOCH_3$	H	16.5	50	>50	>50	>50*	>50*
5o	–	$COOCH_3$	–	H	H	$COOCH_3$	>50*	>50*	>50*	>50*	>50*	>50*
6a	–	COOH	CH_3	–	–	–	>50	>50	>50	>50	>50	>50
6b	–	COOH	C_2H_5	–	–	–	>50	>50	>50	>50	>50	>50
6c	–	COOH	–	H	H	H	>50	>50	>50	>50	>50	>50
7a	–	CH_2OH	CH_3	–	–	–	>50	>50	50	4.6	>50	>50
7b	–	CH_2OH	C_2H_5	–	–	–	>50	>50	50	3.7	>50	>50
7c	–	CH_2OH	–	H	H	H	>50	50	>50	0.24	30.6	>50
7d	–	CH_2OH	–	F	H	H	>50	50	>50	0.43	40.9	>50
7e	–	CH_2OH	–	H	F	H	25	44.0	50	0.59	>50	>50
7f	–	CH_2OH	–	H	H	F	>50	44.2	36.7	0.69	35.9	>50
7g	–	CH_2OH	–	Cl	H	H	16.8	43.1	30.5	5.5	26.7	>50
7h	–	CH_2OH	–	H	Cl	H	14.7	29.8	50	1.1	26.4	>50
7i	–	CH_2OH	–	H	H	Cl	38.9	36.2	31.3	0.79	8.1	44.4
7j	–	CH_2OH	–	OCH_3	H	H	13.3	24.6	30.8	4.3	28.3	60.5
7k	–	CH_2OH	–	H	OCH_3	H	35.4	31.9	52.0	0.33	31.9	>50
7l	–	CH_2OH	–	H	H	OCH_3	54.5	45.9	42.9	0.36	29.8	>50
7m	–	CH_2OH	–	H	$-OCH_2O-$		>50	>50	>50	0.27	>50	>50
7n	–	CH_2OH	–	H	CH_2OH	H	>50	50	>50	0.37	>50	>50
7o	–	CH_2OH	–	H	H	CH_2OH	>50	>50	>50	0.47	>50	>50
9a	O	$COOCH_3$	–	$COOCH_3$	–	–	50*	>50*	>50*	>50*	>50*	>50*
9b	S	$COOCH_3$	–	$COOCH_3$	–	–	>50*	>50*	>50*	>50*	>50*	>50*
9c	Se	$COOCH_3$	–	$COOCH_3$	–	–	>25*	>25*	>25*	>50*	>50*	>25*
10a	O	CH_2OH	–	CH_2OH	–	–	>50	>50	74.1	0.21	31.1	>50
10b	S	CH_2OH	–	CH_2OH	–	–	>50	>50	>50	0.69	>50	>50
10c	Se	CH_2OH	–	CH_2OH	–	–	>50	>50	>50	0.23	>50	>50
YC-1							25.27			0.37		

[a] Human tumor cells were treated with different concentrations of samples for 48 h. Data are presented as IC_{50} (μM, the concentration of 50% proliferation-inhibitory effect).

cell line, and exhibiting low cytotoxicity against the Detroit 551 normal human fetal skin fibroblast cells ($IC_{50} > 50$ μM).

In a different approach, replacement of the CH_2OH group (R_2) of compounds **7a**, **7b**, and **7c** with a $COOCH_3$ group (**5a**, **5b** and **5c**) or with a COOH group (**6a**, **6b** and **6c**) led to reduced inhibitory activity. This finding indicates that the CH_2OH group (R_2) of compounds **7a**, **7b**, and **7c** is a functional group essential for maintaining high inhibitory activity against cancer cells.

Replacement of the benzyl group at the 4-position of compound **7c** with benzyl groups mono-substituted with moieties such as F, Cl, OCH_3, $-OCH_2O-$, or CH_2OH yielded compounds **7d**–**o** that also demonstrated selective inhibitory activity toward the A498 renal cell line (IC_{50} 0.27–5.5 μM). Replacement of the benzyl group at the 4-position of compound **7c** with a 5-(hydroxymethylfuran-2-yl)methyl (**10a**), 5-(hydroxymethylthiophen-2-yl)methyl (**10b**) or 5-(hydroxymethylselenophen-2-yl) methyl group (**10c**) resulted in only minor changes in inhibitory activity against the A498 cell line, with IC_{50} values of 0.21 μM (**10a**), 0.69 μM (**10b**) and 0.24 μM (**10c**), respectively. Alternatively, replacement of the CH_2OH group of compounds **7a**–**o** and **10a**–**c** with a $COOCH_3$ group (**5a**–**o** and **9a**–**c**) significantly attenuated the inhibitory activity of these compounds against the A498 cancer cell line.

In summary, we learned from the previous SARs that the CH_2OH-bearing group on the 2-position and the CH_2–Ar group on the 4-position of the new core skeleton played important roles in boosting the anticancer activity of YC-1 analogs. The compounds **7c**, **10a**, and **10c** exhibited selective inhibitory activity against the A-498 renal cancer cell line and showed improved activity approximately 1.5-fold above that of YC-1. These three compounds warrant further investigation.

2.3. Growth inhibitory activity of *10a* against a panel of human cancer cell lines

We evaluated the inhibitory activity of **10a** against the NCI-60 human tumor cell lines [14,15], and the results are shown in Fig. 1. The mean graph midpoint (MID) values for log GI_{50}, log TGI, and log LC_{50} were −4.57, −4.21, and −4.04, respectively, indicating its relatively low cytotoxicity toward NCI-60 human tumor cell lines. However, we found compound **10a** to demonstrate selective inhibition against NCI-H226 lung cancer, UACC-257 melanoma, OVCAR-5 ovarian cancer, A498 and TK-10 renal cancer and MDA-MB-468 breast cancer cells. In comparison, the log GI_{50}, log TGI, and log LC_{50} values of **10a** against A498 renal cancer cells were −6.85, −6.52, and −6.18, respectively, indicating an approximate 100-fold greater

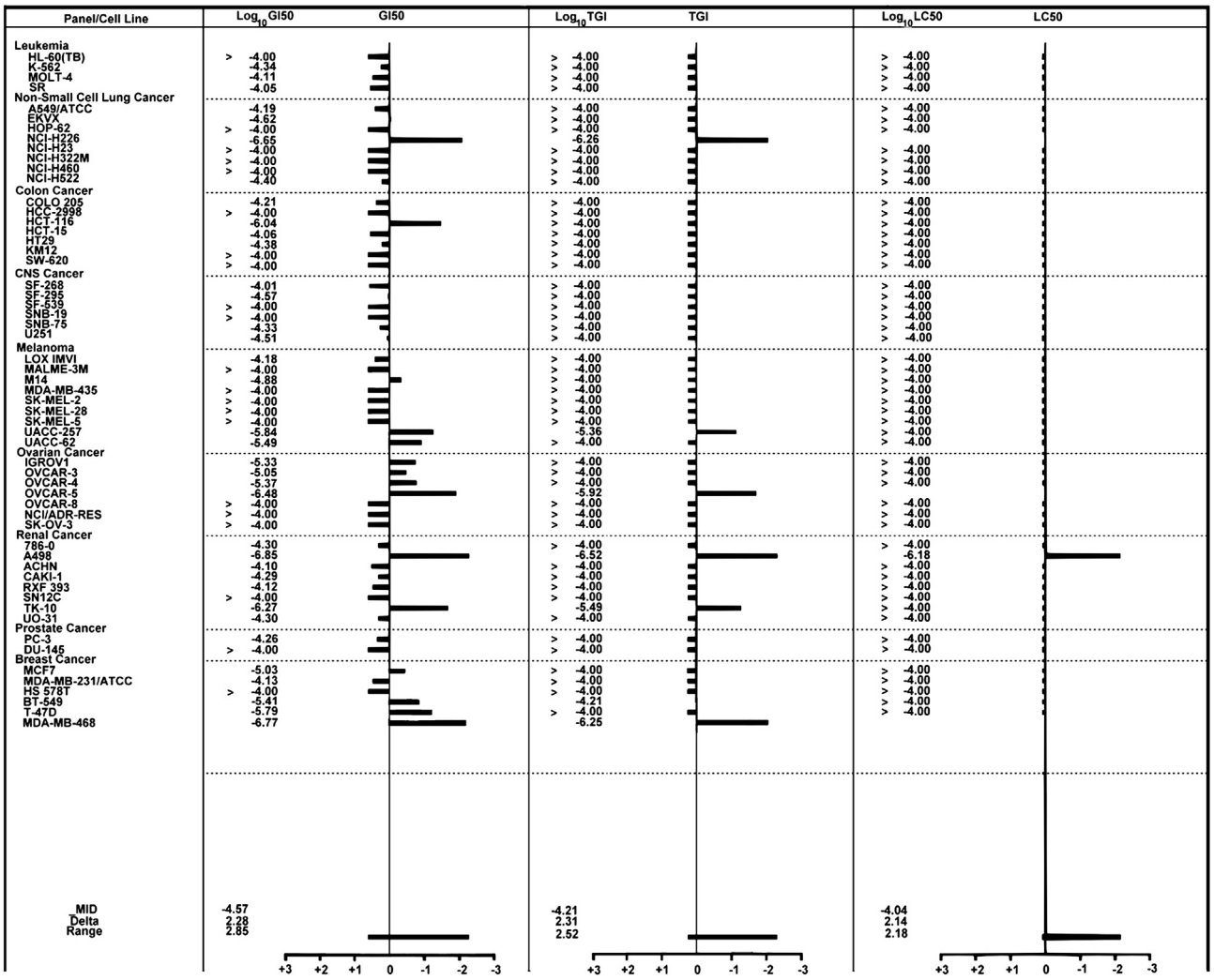

Fig. 1. Differential activity patterns for compound **10a** against 60 human cancer cell lines. MG-MID: mean of log *X* values ($X = GI_{50}$, TGI, and LC_{50}). Delta: logarithm of the difference between the MG-MID and the log *X* of the most sensitive cell line. Range: logarithm of the difference between the log *X* of the most resistant cell line and the log *X* of the most sensitive cell line.

inhibitory potency than that reflected by MID values. Because of its peculiar anticancer selectivity, compound **10a** could serve as a promising lead compound for further investigation.

We then analyzed the differential activity patterns (Fingerprint) of **10a** by using a pattern recognition computer program (COMPARE), which contains a database covering fingerprints from over 175 known anticancer agents with various modes of action. The results of COMPARE analysis at the GI_{50} level for compound **10a** in Table 2 showed a poor correlation ($r < 0.5$) with various known anticancer agents, suggesting that the mode of action of compound **10a** might differ significantly from that of most of the 175 known anticancer agents in the NCI database. However, we observed good similarities ($r = 0.796$) when comparing the anticancer screening fingerprint of **10a** with that of NSC-754549, a YC-1 isostere recently screened by the NCI.

2.4. Mechanism of action of compound *10a*

2.4.1. Toxicity in A498 cells induced by *10a*

Exposure of A498 cells to **10a** for 48 h, followed by MTT metabolism assays, confirmed the effects of **10a** on cell viability. The IC_{50} value was 0.21 μM, and **10a** reduced A498 cell viability in a dose-dependent manner. Exposure of A498 cells to 0.1 μM, 0.25 μM, 0.5 μM, or 1 μM **10a** reduced survival to 82.8 ± 2.8%, 39.5 ± 2.9%, 37.5 ± 1.2%, and 19.4 ± 1.8% of the control (0.1% DMSO), respectively (Fig. 2).

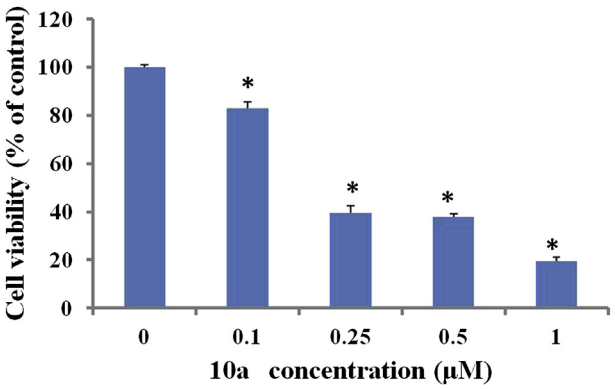

Fig. 2. Effects of **10a** on A498 cell viability. A498 cells were exposed to different concentrations of **10a** for 48 h. Cell viability was assessed using the MTT assay. The data are presented as the mean ± SEM of three independent experiments. Cells without treatment served as a control. *$P < 0.001$ vs. control.

2.4.2. Morphological changes and apoptosis in A498 cells induced by *10a*

Morphological analysis confirmed the cytotoxic effects of **10a**. As shown in Fig. 3A, the apoptotic morphological changes included cell rounding and shrinkage after a 24 h incubation with 0.5 μM of **10a**.

Annexin V-FITC/PI double-labeling was used to detect phosphatidylserine (PS) externalization, a hallmark of the early apoptosis phase (Fig. 3B). Cells incubated in the absence of **10a** for 12 h, 24 h, 36 h, or 48 h were undamaged and were negative for both annexin V-FITC and PI staining (Q3). After incubation with 0.5 μM of **10a** for 24–48 h, the number of advanced apoptotic cells stained positive by annexin V-FITC and negative with PI (Q4) increased significantly with the incubation time. The number of advanced apoptotic cells stained positive by annexin V-FITC and PI (Q2) also increased significantly with the incubation time.

Table 2
COMPARE correlation at the GI_{50} level for compound **10a**.

Compound (NCI number)	r^a	Mechanism of action
O^6-Methylguanine (NSC 37364)	0.316	Alkylating agent [20]
4-Ipomeanol (NSC 349438)	0.291	Alkylating agent [21]
Bruceantin (NSC 165563)	0.197	Inhibition of protein synthesis [22]
Pibenzimol hydrochloride (NSC 322921)	0.183	Inhibition of DNA replication [23]
Mitramycin (NSC 24559)	0.16	Inhibited the synthesis of RNA [24]
Triciribine phosphate (NSC 280594)	0.147	Inhibitor of activation of AKT [25]
Cyanomorpholino-ADR (NSC 357704)	0.143	Alkylating agent [26]
Aclacinomycin A (NSC 208734)	0.139	Stabilizes topoisomerase I cleavage [27]
Chloroquinoxaline sulfonamide (NSC 339004)	0.134	Topoisomerase IIa/b poison [28]
Echinomycin (NSC 526417)	0.133	Inhibitor of RNA synthesis [29]
1-Benzyl-3-(5-hydroxymethyl-2-furyl) selenolo[3,2-*c*]pyrazole (NSC754549)	0.796	YC-1 analog [10]

[a] *r*: correlation coefficient.

During apoptosis, the mitochondrial membrane potential ($\Delta\psi m$) decreased. Cells treatment with 0.5 μM of **10a** for 12 h, 24 h, 36 h, or 48 h, followed by staining with JC-1, confirmed apoptosis as the cause of decreased $\Delta\psi m$. As shown in Fig. 4, in healthy cells with high mitochondrial $\Delta\psi m$, JC-1 spontaneously forms complexes known as the JC-1 polymer (C1 and C2) with intense red fluorescence (0 h). A significant increase occurs in cells with reduced red fluorescence (C3 and C4), indicative of a change in $\Delta\psi m$, in the population in which apoptosis is induced (12–48 h). These data demonstrate that **10a** induces cell apoptosis in A498 cells.

2.4.3. Effects of *10a* on the cell cycle in A498 cells

We treated A498 cells with 0.5 μM of **10a** for 0 h, 24 h, 36 h, or 48 h, followed by flow cytometric analysis to determine the cell-cycle distribution of treated cells. We also investigated whether **10a** disrupts the cell cycle, so that we could provide further insights into the apoptotic effects of this compound. As shown in Fig. 5, **10a** induced a time-dependent accumulation of G_2/M cells and apoptotic (sub-G_1) cells.

To investigate whether G_2/M arrest induced by **10a** was involved in activating cyclin B1 and CDK1, we exposed A498 cells to 0.5 μM of **10a** for 6 h, 12 h, 24 h, 36 h, or 48 h. We then determined the activities of cyclin B1 and CDK1 by using western blot analysis, which revealed the activation of cyclin B1 and CDK1 within 6 h of **10a** treatment (Fig. 6).

2.4.4. Apoptosis induced by *10a* through the activation of mitochondrial signaling pathways in A498 cells

Following our observation that **10a** caused apoptosis in A498 cells, we determined the levels of selected proteins associated with apoptosis. To investigate whether apoptosis induced by **10a** was involved in activating caspase cascades, we exposed A498 cells to 0.5 μM of **10a** for 6 h, 12 h, 24 h, 36 h, or 48 h. The activities of caspase-3 and caspase-9 were then determined using western blot analysis, which revealed the activation of caspase-3 and caspase-9 within 24 h of **10a** treatment. Exposure to **10a** also increased the levels of Endo G, AIF, Apaf-1, and cytochrome *c* (Fig. 7). These results suggest that the mitochondrial signaling pathways of A498 cells mediate **10a**-induced apoptosis.

2.5. In vivo antitumor activity of compound *10a*

We evaluated the target compound **10a** in an A498 xenograft nude mouse model. This compound was delivered intraperitoneally (ip) with doses of 30 mg/kg/d or 60 mg/kg/d. As shown in Fig. 8, compound **10a** significantly suppressed tumor growth in a dose-

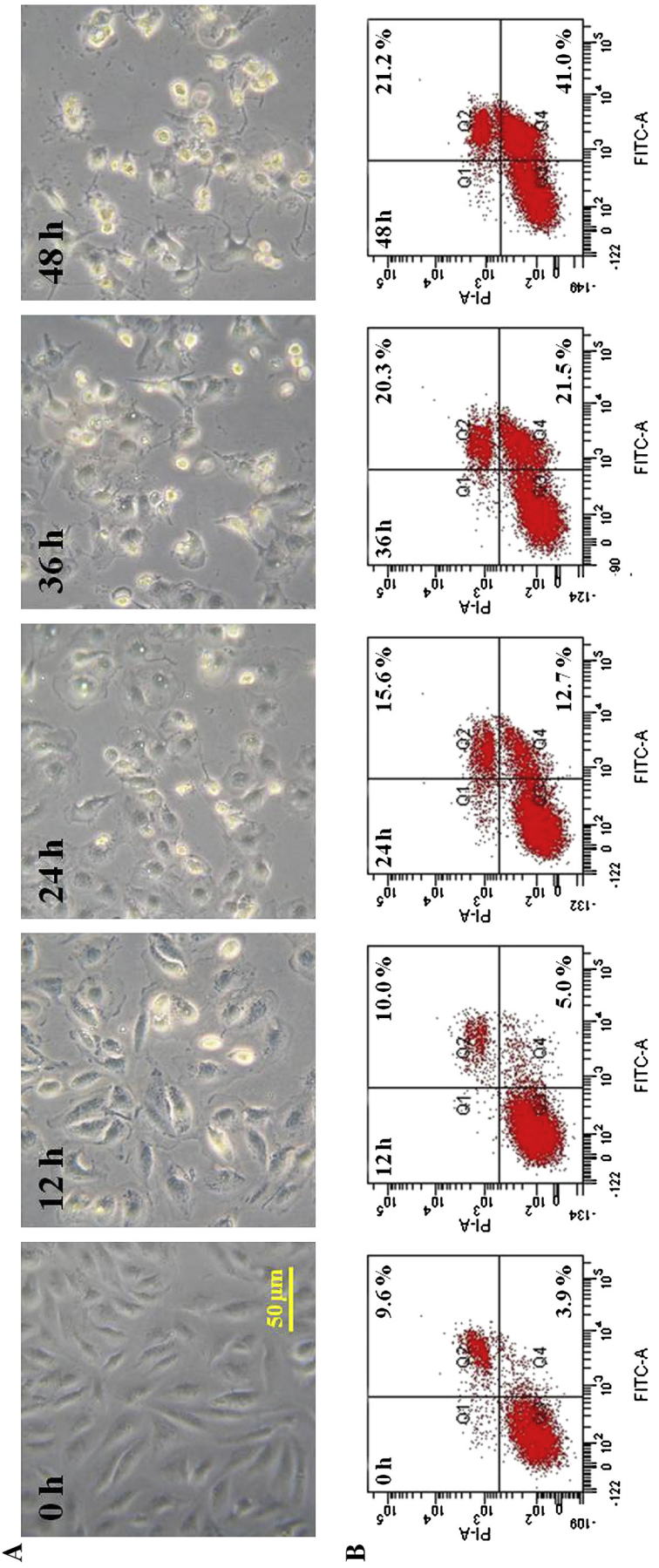

Fig. 3. Morphological changes and apoptosis induced by **10a** in A498 cells. (A) Morphological changes. A498 cells were treated with 0.5 μM **10a** for 12 h, 24 h, 36 h, or 48 h. Cells without treatment served as a control (0 h). Scale bar = 50 μm. (B) Annexin V/PI staining. A498 cells were treated with **10a** for different periods of time and apoptosis was assessed using annexin V/PI staining and flow cytometry. The fraction of annexin V-positive A498 cells was 3.9% prior to treatment and 5.0, 12.7, 21.5 and 41.0% after treatment with A498 cells for 12, 24, 36, or 48 h, respectively.

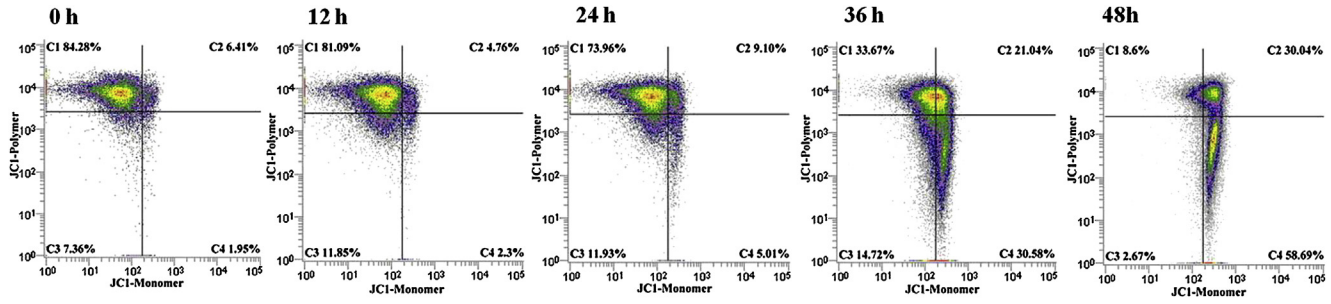

Fig. 4. Effects of **10a** on mitochondrial membrane potential in A498 cells. Cells (1×10^6 cells/mL) were untreated or treated with **10a** (0.5 μM, 12–48 h) to induce apoptosis. Cells were stained with JC-1 according to the protocol on a BD™ MitoScreen as described in the section Methods for staining cells with JC-1 and analyzing by flow cytometry.

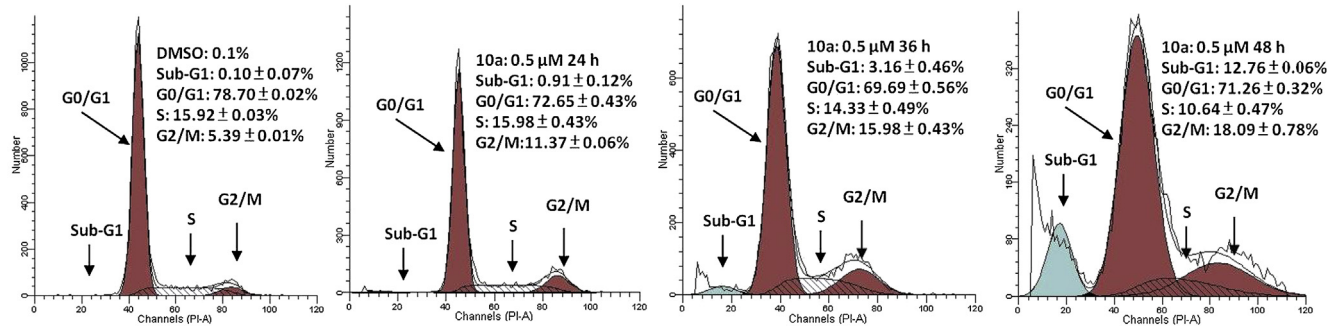

Fig. 5. Effects of **10a** on the cell cycle in A498 cells. A498 cells were incubated with 0.5 μM of **10a** for 0 h, 24 h, 36 h, or 48 h. They were then harvested and analyzed using flow cytometry.

and time-dependent manner. The tumor size was found to decrease by 80% after dosing at 60 mg/kg/d. During the course of the anti-tumor evaluation, no significant body weight changes were detected in either the tested or the control mice.

3. Conclusion

We designed, synthesized, and evaluated a series of 2,4-disubstituted furo[3,2-*b*]indoles *in vitro* for anticancer activity and investigated the SARs of the new YC-1 analogs. Compound **10a**, which demonstrated the best anticancer activity among the tested compounds, was submitted to the NCI for evaluation against the NCI-60 panel of human tumor cell lines. Although compound **10a** contains the furoindole core skeleton, which differs from the selenolopyrazole core skeleton of NSC 754549, the NCI results indicate that the anticancer activity and the fingerprint of **10a** resemble those of 1-benzyl-3-(5-hydroxymethyl-2-furyl)selenolo[3,2-*c*]pyrazole (NSC 754549), a YC-1 isostere. We found that **10a** exhibited greater cytotoxicity against A498 cells compared to YC-1. From the medicinal chemistry viewpoint, compound **10a** presents new possibilities for optimizing YC-1 analogs and warrants further investigation.

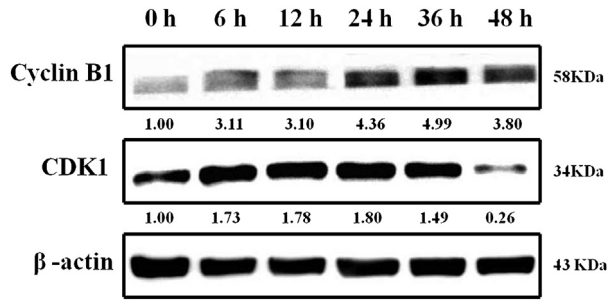

Fig. 6. Treatment with **10a** increased G_2/M phase checkpoint protein expression. A498 cells were treated with 0.5 μM **10a** for the indicated time periods and lysed for protein extraction. Protein samples (20 μg protein/lane) were separated using 10% SDS-PAGE and subjected to immunoblotting with antibodies specific to cyclin B1, CDK1, and β-actin ($n = 3$ independent experiments). β-actin was used as a loading control.

4. Experimental

4.1. Material and physical measurements

All solvents and reagents were obtained commercially and used without further purification. The progress of all reactions was monitored by TLC on 2 cm × 6 cm pre-coated silica gel 60 F_{254} plates, with 0.25 mm thickness (Merck). The chromatograms were visualized under UV light at 254–366 nm. The following adsorbent was used for column chromatography: silica gel 60 (Merck, particle size 0.040–0.063 mm). Melting points (mp) were determined using a Yanaco MP-500D melting point apparatus and were uncorrected. The IR spectra were recorded on Shimadzu IR-Prestige-21 spectrophotometers as KBr pellets. The NMR spectra were recorded on Bruker Avance DPX-200, DPX-400, Bruker Avance III 500 FT-NMR spectrometers and a Varian Unity Inova-600 spectrometer at room temperature, and chemical shifts were reported in parts per million (δ). The following abbreviations were used: s, singlet; d, doublet; t, triplet; q, quartet; dd, double doublet; td, triple doublet; and m, multiplet. Low- and high-resolution mass spectra were performed using Finnigan/Thermo Qust MAT95XL at National Chung Hsing University, Taichung, Taiwan.

4.2. Chemistry

4.2.1. General procedure for synthesizing 4-substituted methyl 4H-furo[3,2-b]indole-2-carboxylate (**5a–o**, **9a–c**)

A mixture of 4*H*-furo[3,2-*b*]indole-2-carboxylate (1 equiv) and NaH (3 equiv, 60%) in anhydrous DMF (5 mL) was stirred for 5 min

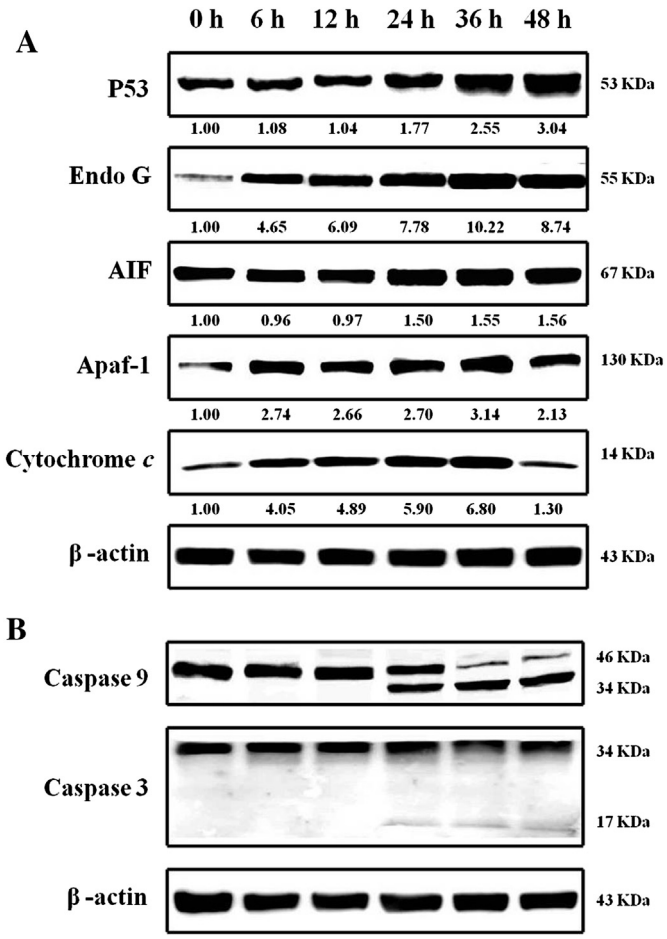

Fig. 7. Treatment with **10a** induced apoptotic pathways in A498 cells. A498 cells were treated with 0.5 μM **10a** for the indicated times and lysed for protein extraction. Protein samples (20 μg protein/lane) were separated using 10% SDS-PAGE and subjected to immunoblotting with antibodies specific to p53, AIF, Endo G, Apaf-1, cytochrome *c*, caspase 9, caspase 3, and β-actin ($n = 3$ independent experiments). β-actin was used as a loading control.

at room temperature. A substituted-benzyl halide or heteroarylmethyl halide (4 equiv) was then added dropwise. The mixture was stirred at room temperature for 20 min. To this mixture was added 50 mL of ice cold water, and the solution was extracted with EtOAc. The organic phase was separately dried over anhydrous $MgSO_4$, filtered, and evaporated under vacuum. The residue was purified by column chromatography on silica gel eluted with EtOAc:*n*-hexane (1:3, v/v) and then recrystallized from *n*-hexane/EtOAc to obtain the pure compound (**5a**–**o**, **9a**–**c**).

*4.2.1.1. Methyl 4-methyl-4H-furo[3,2-b]indole-2-carboxylate (**5a**).* Yield: 51%; white needle crystals; mp: 135–136 °C; IR (KBr) ν (cm^{-1}): 1716 (C═O); ^{1}H NMR (400 MHz, DMSO-d_6) δ (ppm): 3.85 (s, 3H), 3.88 (s, 3H), 7.19 (t, $J = 7.6$ Hz, 1H), 7.35 (t, $J = 7.6$ Hz, 1H), 7.58 (d, $J = 8.4$ Hz, 1H), 7.75 (s, 1H), 7.81 (d, $J = 7.6$ Hz, 1H); ^{13}C NMR (50 MHz, DMSO-d_6) δ (ppm): 31.45, 52.26, 106.39, 111.31, 112.46, 117.67, 120.03, 124.23, 133.07, 142.49, 143.01, 145.75, 159.44; MS (EI, 70 eV) *m*/*z*: 229.1 (M^+); HRMS (EI) *m*/*z*: calc. for $C_{13}H_{11}NO_3$: 229.0739; found: 229.0743.

*4.2.1.2. Methyl 4-ethyl-4H-furo[3,2-b]indole-2-carboxylate (**5b**).* Yield: 28%; white cubic crystals; mp: 122–123 °C; IR (KBr) ν (cm^{-1}): 1714 (C═O); ^{1}H NMR (400 MHz, DMSO-d_6) δ (ppm): 1.38 (t, $J = 7.2$ Hz, 3H), 3.88 (s, 3H), 4.33 (q, $J = 7.2$ Hz, 2H), 7.18 (t, $J = 7.6$ Hz, 1H), 7.34 (t, $J = 8.0$ Hz, 1H), 7.63 (d, $J = 8.4$ Hz, 1H), 7.78 (s, 1H), 7.81 (d, $J = 8.0$ Hz, 1H); ^{13}C NMR (50 MHz, DMSO-d_6) δ (ppm): 14.91, 52.27, 106.73, 111.39, 112.52, 117.79, 120.01, 124.26, 131.75, 141.56, 143.40, 145.76, 159.46; MS (EI, 70 eV) *m*/*z*: 243.1 (M^+); HRMS (EI) *m*/*z*: calc. for $C_{14}H_{13}NO_3$: 243.0895; found: 243.0891.

*4.2.1.3. Methyl 4-benzyl-4H-furo[3,2-b]indole-2-carboxylate (**5c**).* Yield: 36%; white cubic crystals; mp: 168–170 °C; IR (KBr) ν (cm^{-1}): 1718 (C═O); ^{1}H NMR (400 MHz, DMSO-d_6) δ (ppm): 3.86 (s, 3H), 5.53 (s, 2H), 7.19 (t, $J = 7.6$ Hz, 1H), 7.27–7.35 (m, 6H), 7.61 (s, 1H), 7.71 (d, $J = 8.4$ Hz, 1H), 7.83 (d, $J = 8.0$ Hz, 1H); ^{13}C NMR (50 MHz, DMSO-d_6) δ (ppm): 48.24, 106.67, 111.87, 112.79, 117.84, 120.36, 124.47, 127.99, 129.10, 132.34, 137.76, 141.90, 145.83, 159.38; MS (EI, 70 eV) *m*/*z*: 305.2 (M^+); HRMS (EI) *m*/*z*: calc. for $C_{19}H_{15}NO_3$: 305.1052; found: 305.1050.

*4.2.1.4. Methyl 4-(2-fluorobenzyl)-4H-furo[3,2-b]indole-2-carboxylate (**5d**).* Yield: 38%; pale yellow flocculence crystals; mp: 136–138 °C; IR (KBr) ν (cm^{-1}): 1708 (C═O); ^{1}H NMR (500 MHz, DMSO-d_6) δ (ppm): 3.87 (s, 3H), 5.60 (s, 2H), 7.15 (td, $J = 7.4$, 1.1 Hz, 1H), 7.19–7.24 (m, 2H), 7.28 (td, $J = 7.7$, 1.4 Hz, 1H), 7.32–7.38 (m, 2H), 7.54 (s, 1H), 7.70 (d, $J = 8.5$ Hz, 1H), 7.83 (d, $J = 8.0$ Hz, 1H); ^{13}C NMR (125 MHz, DMSO-d_6) δ (ppm): 42.61, 52.33, 106.62, 111.76, 112.84, 116.05 (d, $J = 21.3$ Hz), 117.88, 120.50, 124.44 (d, $J = 26.3$ Hz), 124.46, 125.18 (d, $J = 3.8$ Hz), 130.59 (d, $J = 8.8$ Hz), 130.65, 132.25, 141.86, 143.48, 145.87, 159.36, 160.72 (d, $J = 243.8$ Hz); MS (EI, 70 eV) *m*/*z*: 323.1 (M^+); HRMS (EI) *m*/*z*: calc. for $C_{19}H_{14}FNO_3$: 323.0958; found: 323.0952.

*4.2.1.5. Methyl 4-(3-fluorobenzyl)-4H-furo[3,2-b]indole-2-carboxylate (**5e**).* Yield: 46%; white flocculence crystals; mp: 160–162 °C; IR (KBr) ν (cm^{-1}): 1708 (C═O); ^{1}H NMR (500 MHz, DMSO-d_6) δ (ppm): 3.87 (s, 3H), 5.57 (s, 2H), 7.09–7.16 (m, 3H), 7.20 (t, $J = 7.0$ Hz, 1H), 7.33–7.38 (m, 2H), 7.71 (s, 1H), 7.72 (d, $J = 6.0$ Hz, 1H), 7.84 (d, $J = 8.0$ Hz, 1H); ^{13}C NMR (125 MHz, DMSO-d_6) δ (ppm): 47.68, 52.32, 106.67, 111.85, 112.93, 114.66, 114.93 (d, $J = 21.3$ Hz), 117.92, 120.52, 123.94, 124.57, 131.20 (d, $J = 7.5$ Hz), 132.37, 140.75, 141.89, 143.51, 145.97, 159.38, 162.65 (d, $J = 242.5$ Hz); MS (EI, 70 eV) *m*/*z*: 323.2 (M^+); HRMS (EI) *m*/*z*: calc. for $C_{19}H_{14}FNO_3$: 323.0958; found: 323.0951.

*4.2.1.6. Methyl 4-(4-fluorobenzyl)-4H-furo[3,2-b]indole-2-carboxylate (**5f**).* Yield: 56%; white cubic crystals; mp: 175–177 °C; IR (KBr) ν (cm^{-1}): 1718 (C═O); ^{1}H NMR (500 MHz, DMSO-d_6) δ (ppm): 3.87 (s, 3H), 5.53 (s, 2H), 7.12–7.17 (m, 2H), 7.20 (td, $J = 7.2$, 1.0 Hz, 1H), 7.32–7.38 (m, 3H), 7.66 (s, 1H), 7.72 (d, $J = 8.5$ Hz, 1H), 7.82 (d, $J = 7.7$ Hz, 1H); ^{13}C NMR (125 MHz, DMSO-d_6) δ (ppm): 47.48, 52.32, 106.68, 111.87, 112.88, 115.93 (d, $J = 21.3$ Hz), 117.89, 120.43, 124.52, 130.14 (d, $J = 8.8$ Hz), 132.26, 134.08, 141.84, 143.51, 145.91, 159.39, 162.05 (d, $J = 242.5$ Hz); MS (EI, 70 eV) *m*/*z*: 323.1 (M^+); HRMS (EI) *m*/*z*: calc. for $C_{19}H_{14}FNO_3$: 323.0958; found: 323.0963.

*4.2.1.7. Methyl 4-(2-chlorobenzyl)-4H-furo[3,2-b]indole-2-carboxylate (**5g**).* Yield: 42%; yellow needle crystals; mp: 157–159 °C; IR (KBr) ν (cm^{-1}): 1708 (C═O); ^{1}H NMR (400 MHz, DMSO-d_6) δ (ppm): 3.85 (s, 3H), 5.62 (s, 2H), 6.99 (d, $J = 7.2$ Hz, 1H), 7.21 (d, $J = 7.4$ Hz, 1H), 7.28 (d, $J = 7.4$ Hz, 1H), 7.31–7.36 (m, 3H), 7.53 (d, $J = 8.0$ Hz, 1H), 7.60 (d, $J = 8.4$ Hz, 1H), 7.86 (d, $J = 8.0$ Hz, 1H); ^{13}C NMR (50 MHz, DMSO-d_6) δ (ppm): 46.44, 52.34, 106.53, 111.75, 112.79, 117.90, 120.59, 124.64, 128.05, 129.88, 130.15, 132.23, 134.65, 142.02, 143.50, 145.79, 159.34; MS (EI, 70 eV) *m*/*z*: 339.1 (M^+); HRMS (EI) *m*/*z*: calc. for $C_{19}H_{14}ClNO_3$: 339.0662; found: 339.0658.

*4.2.1.8. Methyl 4-(3-chlorobenzyl)-4H-furo[3,2-b]indole-2-carboxylate (**5h**).* Yield: 25%; yellow crystals; mp: 135–137 °C; IR (KBr) ν (cm^{-1}): 1710 (C═O); ^{1}H NMR (400 MHz, DMSO-d_6) δ (ppm): 3.87 (s, 3H), 5.55 (s, 2H), 7.18–7.38 (m, 6H), 7.70 (d, $J = 6.0$ Hz, 1H), 7.71 (s,

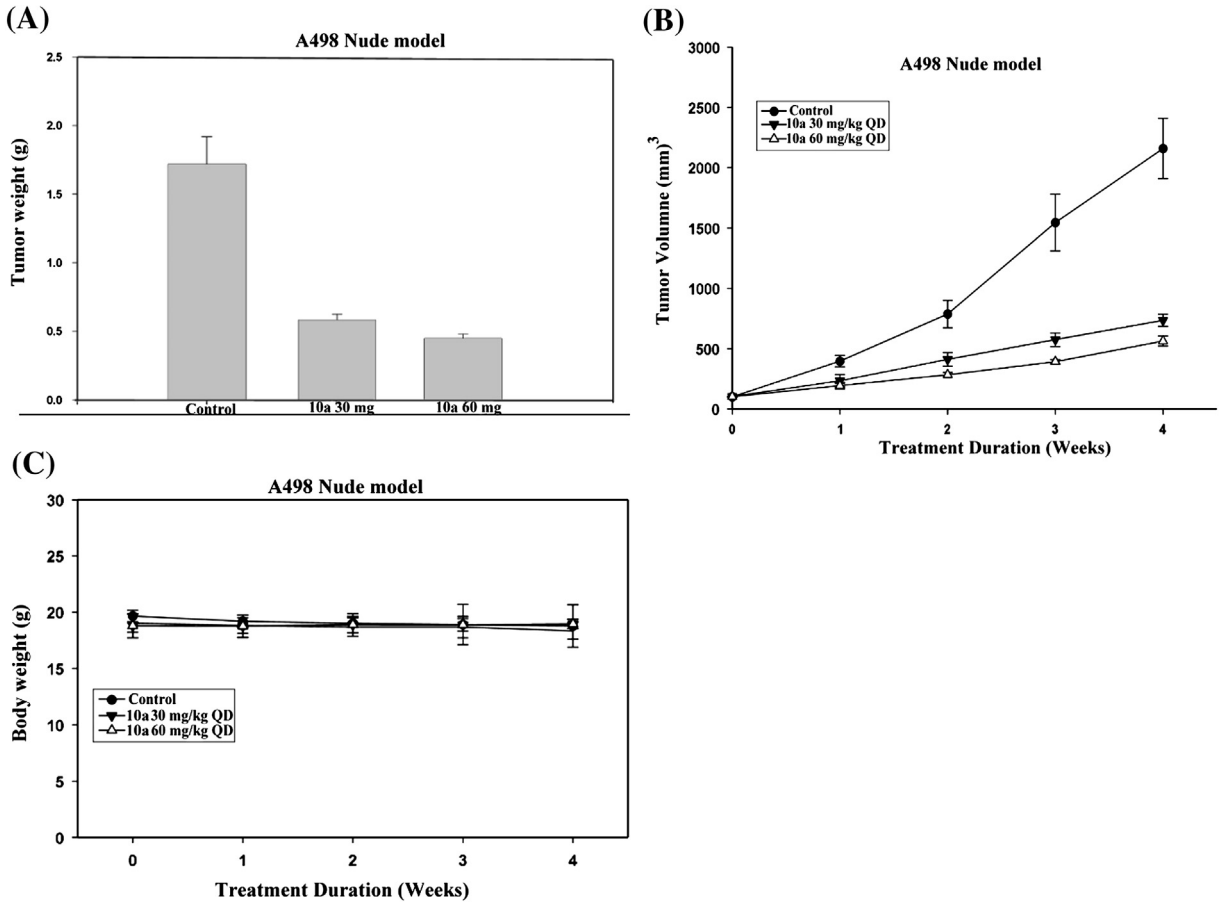

Fig. 8. Effect of **10a** on tumor cell growth in an *in vivo* model. (A) Mean tumor weight–time profiles. (B) Mean tumor volume–time profiles, and (C) Mean body weight–time profiles in A498 xenograft nude mice ($n = 5$) following ip dosing of **10a** at 30 mg/kg or 60 mg/kg QD for 4 consecutive weeks.

1H), 7.83 (d, $J = 8.0$ Hz, 1H); ^{13}C NMR (50 MHz, DMSO-d_6) δ (ppm): 47.49, 52.36, 106.50, 111.70, 112.81, 117.86, 120.62, 124.69, 126.42, 127.50, 128.08, 131.05, 132.19, 133.67, 140.24, 141.80, 143.49, 145.90, 159.46; MS (EI, 70 eV) *m*/*z*: 339.1 (M^+); HRMS (EI) *m*/*z*: calc. for $C_{19}H_{14}ClNO_3$: 339.0662; found: 339.0670.

*4.2.1.9. Methyl 4-(4-chlorobenzyl)-4H-furo[3,2-b]indole-2-carboxylate (**5i**).* Yield: 64%; pale yellow cubic crystals; mp: 152–154 °C; IR (KBr) ν (cm^{-1}): 1718 (C=O); ^{1}H NMR (400 MHz, DMSO-d_6) δ (ppm): 3.87 (s, 3H), 5.54 (s, 2H), 7.19 (t, $J = 7.2$ Hz, 1H), 7.30 (d, $J = 8.4$ Hz, 2H), 7.33 (t, $J = 8.0$ Hz, 1H), 7.38 (d, $J = 8.4$ Hz, 2H), 7.69 (*s*, 1H), 7.70 (d, $J = 9.2$ Hz, 1H), 7.83 (d, $J = 8.0$ Hz, 1H); ^{13}C NMR (50 MHz, DMSO-d_6) δ (ppm): 47.45, 52.32, 106.62, 111.80, 112.86, 117.88, 120.48, 124.54, 129.08, 129.76, 132.26, 132.70, 136.82, 141.81, 143.48, 145.89, 159.37; MS (EI, 70 eV) *m*/*z*: 339.1 (M^+); HRMS (EI) *m*/*z*: calc. for $C_{19}H_{14}ClNO_3$: 339.0662; found: 339.0672.

*4.2.1.10. Methyl 4-(2-methoxybenzyl)-4H-furo[3,2-b]indole-2-carboxylate (**5j**).* Yield: 33%; white crystals; mp: 124–126 °C; IR (KBr) ν (cm^{-1}): 1714 (C=O); ^{1}H NMR (400 MHz, DMSO-d_6) δ (ppm): 3.78 (s, 3H), 3.86 (s, 3H), 5.45 (s, 2H), 6.87 (t, $J = 7.2$ Hz, 1H), 7.03 (d, $J = 8.4$ Hz, 1H), 7.07 (d, $J = 6.4$ Hz, 1H), 7.17 (t, $J = 7.2$ Hz, 1H), 7.27–7.33 (m, 2H), 7.42 (s, 1H), 7.64 (d, $J = 8.4$ Hz, 1H), 7.81 (d, $J = 8.0$ Hz, 1H); ^{13}C NMR (50 MHz, DMSO-d_6) δ (ppm): 43.87, 52.28, 55.81, 106.72, 111.46, 111.87, 112.60, 117.72, 120.18, 120.80, 124.32, 125.04, 129.53, 129.81, 132.48, 141.94, 143.26, 145.67, 157.49, 159.40; MS (EI, 70 eV) *m*/*z*: 335.2 (M^+); HRMS (EI) *m*/*z*: calc. for $C_{20}H_{17}NO_4$: 335.1158; found: 335.1165.

*4.2.1.11. Methyl 4-(3-methoxybenzyl)-4H-furo[3,2-b]indole-2-carboxylate (**5k**).* Yield: 58%; brown crystals; mp: 71–73 °C; IR (KBr) ν (cm^{-1}): 1716 (C=O); ^{1}H NMR (400 MHz, DMSO-d_6) δ (ppm): 3.74 (s, 3H), 3.85 (s, 3H), 5.48 (s, 2H), 6.79–7.34 (m, 6H), 7.62 (s, 1H), 7.69 (d, $J = 8.4$ Hz, 1H), 7.82 (d, $J = 8.0$ Hz, 1H); ^{13}C NMR (50 MHz, DMSO-d_6) δ (ppm): 48.12, 52.31, 55.43, 106.65, 111.87, 112.77, 113.03, 113.98, 114.12, 114.24, 117.83, 119.99, 120.39, 124.49, 130.26, 132.37, 139.33, 141.92, 145.84, 159.79; MS (EI, 70 eV) *m*/*z*: 335.2 (M^+); HRMS (EI) *m*/*z*: calc. for $C_{20}H_{17}NO_4$: 335.1158; found: 335.1160.

*4.2.1.12. Methyl 4-(4-methoxybenzyl)-4H-furo[3,2-b]indole-2-carboxylate (**5l**).* Yield: 43%; white needle crystals; mp: 88–90 °C; IR (KBr) ν (cm^{-1}): 1714 (C=O); ^{1}H NMR (400 MHz, DMSO-d_6) δ (ppm): 3.69 (s, 3H), 3.85 (s, 3H), 5.43 (s, 2H), 6.87 (d, $J = 8.4$ Hz, 2H), 7.18 (t, $J = 7.6$ Hz, 1H), 7.26 (d, $J = 8.4$ Hz, 2H), 7.33 (t, $J = 7.6$ Hz, 1H), 7.57 (s, 1H), 7.72 (d, $J = 8.4$ Hz, 1H), 7.80 (d, $J = 8.0$ Hz, 1H); ^{13}C NMR (50 MHz, DMSO-d_6) δ (ppm): 47.71, 52.31, 55.46, 106.66, 111.85, 112.72, 114.41, 117.79, 120.30, 124.44, 129.54, 130.83, 132.15, 141.81, 143.45, 145.77, 159.18, 159.41; MS (EI, 70 eV) *m*/*z*: 335.2 (M^+); HRMS (EI) *m*/*z*: calc. for $C_{20}H_{17}NO_4$: 335.1158; found: 335.1162.

*4.2.1.13. Methyl 4-(3,4-(methylenedioxy)benzyl)-4H-furo[3,2-b]indole-2-carboxylate (**5m**).* Yield: 42%; white flocculence crystals; mp: 96–98 °C; IR (KBr) ν (cm^{-1}): 1706 (C=O); ^{1}H NMR (400 MHz, DMSO-d_6) δ (ppm): 3.87 (s, 3H), 5.42 (s, 2H), 5.97 (s, 2H), 6.85 (s, 2H), 6.91 (s, 1H), 7.19 (t, $J = 7.6$ Hz, 1H), 7.34 (t, $J = 8.0$ Hz, 1H), 7.68 (s, 1H), 7.75 (d,

J = 8.4 Hz, 1H), 7.82 (d, J = 8.0 Hz, 1H); ^{13}C NMR (50 MHz, DMSO-d_6) δ (ppm): 48.05, 52.30, 101.49, 106.76, 108.68, 108.76, 111.95, 112.82, 117.84, 120.33, 121.67, 124.44, 131.52, 132.21, 141.80, 143.47, 145.85, 147.20, 147.84, 159.39; MS (EI, 70 eV) m/z: 349.1 (M^+); HRMS (EI) m/z: calc. for $C_{20}H_{15}NO_5$: 349.0950; found: 349.0946.

*4.2.1.14. Methyl 4-(3-(methoxycarbonyl)benzyl)-4H-furo[3,2-b]indole-2-carboxylate (**5n**).* Yield: 36%; pale yellow flocculence crystals; mp: 132–133 °C; IR (KBr) ν (cm^{-1}): 1695 (C=O), 1726 (C=O); ^{1}H NMR (400 MHz, DMSO-d_6) δ (ppm): 3.81 (s, 3H), 3.86 (s, 3H), 5.64 (s, 2H), 7.20 (t, J = 7.2 Hz, 1H), 7.33 (t, J = 7.6 Hz, 1H), 7.47 (t, J = 7.6 Hz, 1H), 7.52 (d, J = 7.6 Hz, 1H), 7.66 (s, 1H), 7.69 (d, J = 8.4 Hz, 1H), 7.84 (d, J = 7.6 Hz, 1H), 7.86 (d, J = 7.2 Hz, 1H), 7.90 (s, 1H); ^{13}C NMR (50 MHz, DMSO-d_6) δ (ppm): 47.74, 52.32, 52.65, 106.56, 111.76, 112.87, 117.90, 120.53, 124.60, 128.34, 128.86, 129.67, 130.43, 132.33, 132.64, 138.66, 141.89, 143.49, 145.92, 159.37, 166.42; MS (EI, 70 eV) m/z: 363.2 (M^+); HRMS (EI) m/z: calc. for $C_{21}H_{17}NO_5$: 363.1107; found: 363.1099.

*4.2.1.15. Methyl 4-(4-(methoxycarbonyl)benzyl)-4H-furo[3,2-b]indole-2-carboxylate (**5o**).* Yield: 47%; white crystals; mp: 142–144 °C; IR (KBr) ν (cm^{-1}): 1701 (C=O), 1716 (C=O); ^{1}H NMR (400 MHz, DMSO-d_6) δ (ppm): 3.82 (s, 3H), 3.86 (s, 3H), 5.65 (s, 2H), 7.20 (t, J = 7.6 Hz, 1H), 7.32 (t, J = 8.0 Hz, 1H), 7.38 (d, J = 8.0 Hz, 2H), 7.66 (d, J = 10.0 Hz, 1H), 7.67 (s, 1H), 7.84 (d, J = 8.0 Hz, 1H), 7.90 (d, J = 8.4 Hz, 2H); ^{13}C NMR (50 MHz, DMSO-d_6) δ (ppm): 47.86, 52.32, 52.57, 106.64, 111.79, 112.89, 117.92, 120.53, 124.58, 128.01, 129.33, 130.02, 132.40, 141.89, 143.29, 143.48, 145.91, 159.37, 166.35; MS (EI, 70 eV) m/z: 363.1 (M^+); HRMS (EI) m/z: calc. for $C_{21}H_{17}NO_5$: 363.1107; found: 363.1115.

*4.2.1.16. Methyl 4-((5-(methoxycarbonyl)furan-2-yl)methyl)-4H-furo[3,2-b]indole-2-carboxylate (**9a**).* Yield: 37%; pale yellow cubic crystals; mp: 141–143 °C; IR (KBr) ν (cm^{-1}): 1707 (C=O), 1728 (C=O), 2954 (CH); ^{1}H NMR (400 MHz, DMSO-d_6) δ (ppm): 3.75 (s, 3H), 3.88 (s, 3H), 5.66 (s, 2H), 6.68 (d, J = 3.6 Hz, 1H), 7.22 (t, J = 7.6 Hz, 1H), 7.24 (d, J = 3.6 Hz, 1H), 7.37 (t, J = 7.6 Hz, 1H), 7.66 (s, 1H), 7.77 (d, J = 8.4 Hz, 1H), 7.83 (d, J = 8.0 Hz, 1H); ^{13}C NMR (50 MHz, DMSO-d_6) δ (ppm): 52.24, 52.34, 106.62, 111.55, 111.76, 113.00, 117.89, 119.66, 120.70, 124.62, 132.13, 141.87, 143.59, 144.00, 145.94, 155.32, 158.52, 159.34; MS (EI, 70 eV) m/z: 353.1 (M^+); HRMS (EI) m/z: calc. for $C_{19}H_{15}NO_6$: 353.0899; found: 353.0890.

*4.2.1.17. Methyl 4-((5-(methoxycarbonyl)thiophen-2-yl)methyl)-4H-furo[3,2-b]indole -2-carboxylate (**9b**).* Yield: 35%; pale yellow crystals; mp: 140–142 °C; IR (KBr) ν (cm^{-1}): 1726 (C=O); ^{1}H NMR (400 MHz, DMSO-d_6) δ (ppm): 3.74 (s, 3H), 3.88 (s, 3H), 5.82 (s, 2H), 7.22 (t, J = 7.6 Hz, 1H), 7.26 (d, J = 3.6 Hz, 1H), 7.37 (t, J = 8.0 Hz, 1H), 7.65 (d, J = 3.6 Hz, 1H), 7.78 (s, 1H), 7.79 (d, J = 8.8 Hz, 1H), 7.83 (d, J = 8.0 Hz, 1H); ^{13}C NMR (50 MHz, DMSO-d_6) δ (ppm): 43.16, 52.36, 52.64, 106.74, 111.90, 113.24, 117.99, 120.82, 124.67, 128.25, 132.00, 132.44, 134.08, 141.72, 143.79, 146.02, 147.97, 159.34, 161.97; MS (EI, 70 eV) m/z: 369.1 (M^+); HRMS (EI) m/z: calc. for $C_{19}H_{15}NO_5S$: 369.0671; found: 369.0677.

*4.2.1.18. Methyl 4-((5-(methoxycarbonyl)selenophen-2-yl)methyl)-4H-furo[3,2-b]indole-2-carboxylate (**9c**).* Yield: 34%; pale yellow crystals; mp: 129–131 °C; IR (KBr) ν (cm^{-1}): 1701 (C=O); ^{1}H NMR (400 MHz, DMSO-d_6) δ (ppm): 3.72 (s, 3H), 3.87 (s, 3H), 5.83 (s, 2H), 7.21–7.86 (m, 7H); ^{13}C NMR (50 MHz, DMSO-d_6) δ (ppm): 45.44, 52.36, 52.75, 106.73, 111.88, 113.28, 117.98, 120.87, 124.70, 130.21, 131.92, 136.34, 137.73, 141.73, 143.89, 145.99, 155.34, 159.36, 163.29; MS (EI, 70 eV) m/z: 417.1 (M^+); HRMS (EI) m/z: calc. for $C_{19}H_{15}NO_5Se$: 417.0115; found: 411.0110.

*4.2.2. General procedure for synthesizing 4-substituted 4H-furo[3,2-b]indole-2-carboxylic acid (**3**, **6a**–**c**)*

Compound (**1**, **5a**–**c**) (1 equiv) was dissolved in 20 mL of a 10% sodium hydroxide solution. The mixture was heated under reflux for 2 h and then cooled and acidified with dilute HCl. The precipitate was collected and recrystallized from *n*-hexane/EtOAc to yield the pure compound (**3**, **6a**–**c**).

*4.2.2.1. 4H-Furo[3,2-b]indole-2-carboxylic acid (**3**).* Yield: 66%; pale yellow crystals; mp: 242–243 °C; IR (KBr) ν (cm^{-1}): 1672 (C=O), 3427 (OH); ^{1}H NMR (400 MHz, DMSO-d_6) δ (ppm): 7.15 (t, J = 7.6 Hz, 1H), 7.27 (t, J = 8.0 Hz, 1H), 7.49 (s, 1H), 7.50 (d, J = 10.4 Hz, 1H), 7.78 (d, J = 8.0 Hz, 1H), 11.12 (s, 1H); ^{13}C NMR (50 MHz, DMSO-d_6) δ (ppm): 106.44, 112.67, 113.39, 117.32, 119.95, 123.94, 130.51, 141.99, 144.03, 147.12, 160.51; MS (EI, 70 eV) m/z: 201.1 (M^+); HRMS (EI) m/z: calc. for $C_{11}H_7NO_3$: 201.0426; found: 201.0422.

*4.2.2.2. 4-Methyl-4H-furo[3,2-b]indole-2-carboxylic acid (**6a**).* Yield: 36%; white crystals; mp: 237–239 °C; IR (KBr) ν (cm^{-1}): 1664 (C=O); ^{1}H NMR (400 MHz, DMSO-d_6) δ (ppm): 3.86 (s, 3H), 7.18 (t, J = 7.2 Hz, 1H), 7.33 (t, J = 7.6 Hz, 1H), 7.58 (d, J = 8.4 Hz, 1H), 7.64 (s, 1H), 7.79 (d, J = 8.0 Hz, 1H); ^{13}C NMR (50 MHz, DMSO-d_6) δ (ppm): 31.47, 105.82, 111.26, 112.63, 117.50, 119.93, 123.91, 133.20, 142.23, 142.59, 147.13, 160.43; MS (EI, 70 eV) m/z: 215.1 (M^+); HRMS (EI) m/z: calc. for $C_{12}H_9NO_3$: 215.0582; found: 215.0585.

*4.2.2.3. 4-Ethyl-4H-furo[3,2-b]indole-2-carboxylic acid (**6b**).* Yield: 71%; brown flocculence crystals; mp: 203–205 °C; IR (KBr) ν (cm^{-1}): 1670 (C=O), 3448 (OH); ^{1}H NMR (400 MHz, DMSO-d_6) δ (ppm): 1.37 (t, J = 7.2 Hz, 3H), 4.31 (q, J = 7.2 Hz, 2H), 7.16 (t, J = 7.6 Hz, 1H), 7.31 (t, J = 7.2 Hz, 1H), 7.61 (d, J = 8.4 Hz, 1H), 7.66 (s, 1H), 7.78 (d, J = 8.0 Hz, 1H); ^{13}C NMR (50 MHz, DMSO-d_6) δ (ppm): 14.94, 106.18, 111.33, 112.68, 117.64, 119.92, 123.97, 131.86, 141.31, 143.00, 147.03, 160.43; MS (EI, 70 eV) m/z: 229.1 (M^+); HRMS (EI) m/z: calc. for $C_{13}H_{11}NO_3$: 229.0739; found: 229.0733.

*4.2.2.4. 4-Benzyl-4H-furo[3,2-b]indole-2-carboxylic acid (**6c**).* Yield: 46%; brown cubic crystals; mp: 141–143 °C; IR (KBr) ν (cm^{-1}): 3439 (OH); ^{1}H NMR (400 MHz, DMSO-d_6) δ (ppm): 5.52 (s, 2H), 7.18 (t, J = 7.6 Hz, 1H), 7.25–7.34 (m, 6H), 7.48 (s, 1H), 7.69 (d, J = 8.4 Hz, 1H), 7.80 (d, J = 8.0 Hz, 1H); ^{13}C NMR (50 MHz, DMSO-d_6) δ (ppm): 48.24, 106.11, 111.79, 112.96, 117.66, 120.24, 124.12, 127.99, 129.09, 132.47, 137.84, 141.66, 143.01, 147.17, 160.33; MS (EI, 70 eV) m/z: 291.10 (M^+); HRMS (EI) m/z: calc. for $C_{18}H_{13}NO_3$: 291.0895; found: 291.0893.

*4.2.3. General procedure for synthesizing 4-substituted 4H-furo[3,2-b]indole-2-methanol (**7a**–**o**, **10a**–**c**)*

Compound (**5a**–**o**, **9a**–**c**) (1 equiv) was dissolved in a homogenous solution of $Ca(BH_4)_2$ (10 equiv) in THF (50 mL). The mixture was heated under reflux for 10 h and then filtered. The solvent was evaporated, and the residues were extracted with CH_2Cl_2. The organic phase was separated, dried over anhydrous $MgSO_4$, filtered, and evaporated under vacuum. The residues were purified by column chromatography on silica gel eluted with EtOAc:*n*-hexane (1:1, v/v) and then recrystallized from *n*-hexane/EtOAc to obtain the pure compound (**7a**–**o**, **10a**–**c**).

*4.2.3.1. 4H-Furo[3,2-b]indole-2-methanol (**2**).* Yield: 22%; brown needle crystals; mp: 105–107 °C; IR (KBr) ν (cm^{-1}): 3394 (OH); ^{1}H NMR (400 MHz, DMSO-d_6) δ (ppm): 4.53 (d, J = 3.2 Hz, 2H), 5.33 (t, J = 3.2 Hz, 1H), 6.63 (s, 1H), 7.05–7.10 (m, 2H), 7.42 (d, J = 7.6 Hz, 1H), 7.59 (d, J = 7.6 Hz, 1H), 10.79 (s, 1H); ^{13}C NMR (50 MHz, DMSO-d_6) δ (ppm): 57.25, 97.71, 112.92, 113.68, 115.51, 119.28, 121.16, 131.22, 139.54, 140.51, 159.58; MS (EI, 70 eV) m/z: 187.1 (M^+); HRMS (EI) m/z: calc. for $C_{11}H_9NO_2$: 187.0633; found: 187.0627.

*4.2.3.2. 4-Methyl-4H-furo[3,2-b]indole-2-methanol (**7a**).* Yield: 54%; brown oil; IR (KBr) ν (cm^{-1}): 2924 (CH), 3448 (OH); ^1H NMR (400 MHz, DMSO-d_6) δ (ppm): 3.80 (s, 3H), 4.55 (d, J = 4 Hz, 2H), 5.38 (s, 1H), 6.75 (s, 1H), 7.09 (t, J = 7.2 Hz, 1H), 7.17 (t, J = 7.2 Hz, 1H), 7.49 (d, J = 8.0 Hz, 1H), 7.61 (d, J = 8.0 Hz, 1H); ^{13}C NMR (50 MHz, DMSO-d_6) δ (ppm): 31.44, 57.28, 96.90, 110.79, 113.58, 115.70, 119.29, 121.14, 134.01, 139.17, 139.85, 159.75; MS (EI, 70 eV) m/z: 201.0 (M^+); HRMS (EI) m/z: calc. for $C_{12}H_{11}NO$: 201.0790; found: 201.0787.

*4.2.3.3. 4-Ethyl-4H-furo[3,2-b]indole-2-methanol (**7b**).* Yield: 63%; brown oil; IR (KBr) ν (cm^{-1}): 2924 (CH), 3417 (OH); ^1H NMR (400 MHz, DMSO-d_6) δ (ppm): 1.36 (t, J = 7.2 Hz, 3H), 4.27 (q, J = 7.2 Hz, 2H), 4.55 (d, J = 5.6 Hz, 2H), 5.37 (t, J = 5.6 Hz, 1H), 6.78 (s, 1H), 7.08 (t, J = 7.6 Hz, 1H), 7.16 (t, J = 7.2 Hz, 1H), 7.53 (d, J = 8.0 Hz, 1H), 7.61 (d, J = 7.6 Hz, 1H); ^{13}C NMR (50 MHz, DMSO-d_6) δ (ppm): 15.03, 57.25, 97.31, 110.82, 113.62, 115.80, 119.22, 121.15, 132.61, 138.87, 139.55, 159.65; MS (EI, 70 eV) m/z: 215.0 (M^+); HRMS (EI) m/z: calc. for $C_{13}H_{13}NO_2$: 215.0946; found: 215.0949.

*4.2.3.4. 4-Benzyl-4H-furo[3,2-b]indole-2-methanol (**7c**).* Yield: 62%; brown oil; IR (KBr) ν (cm^{-1}): 2924 (CH), 3454 (OH); ^1H NMR (400 MHz, DMSO-d_6) δ (ppm): 4.52 (d, J = 5.2 Hz, 2H), 5.36 (t, J = 5.2 Hz, 1H), 5.47 (s, 2H), 6.63 (s, 1H), 7.09 (t, J = 7.2 Hz, 1H), 7.15 (t, J = 7.2 Hz, 1H), 7.23–7.32 (m, 5H), 7.61 (d, J = 7.6 Hz, 1H), 7.63 (d, J = 6.8 Hz, 1H); ^{13}C NMR (50 MHz, DMSO-d_6) δ (ppm): 48.20, 57.24, 97.32, 111.29, 113.88, 115.85, 119.58, 121.37, 127.76, 127.89, 129.01, 133.28, 138.28, 139.33, 139.61, 159.78; MS (EI, 70 eV) m/z: 277.2 (M^+); HRMS (EI) m/z: calc. for $C_{18}H_{15}NO_2$: 277.1103; found: 277.1105.

*4.2.3.5. 4-(2-Fluorobenzyl)-4H-furo[3,2-b]indole-2-methanol (**7d**).* Yield: 52%; brown oil; IR (KBr) ν (cm^{-1}): 2924 (CH), 3448 (OH); ^1H NMR (500 MHz, DMSO-d_6) δ (ppm): 4.52 (d, J = 5 Hz, 2H), 5.37 (t, J = 5.5 Hz, 1H), 5.53 (s, 2H), 6.58 (s, 1H), 7.10–7.25 (m, 6H), 7.62 (d, J = 7.0 Hz, 1H), 7.64 (d, J = 6.5 Hz, 1H); ^{13}C NMR (125 MHz, DMSO-d_6) δ (ppm): 42.41, 57.23, 97.32, 111.21, 113.90, 115.89, 115.97 (d, J = 20 Hz), 119.74, 121.49, 124.84 (d, J = 15 Hz), 125.09 (d, J = 2.5 Hz), 130.37 (d, J = 10 Hz), 130.44, 133.12, 139.30, 139.66, 159.79, 160.64 (d, J = 243.8 Hz); MS (EI, 70 eV) m/z: 295.2 (M^+); HRMS (EI) m/z: calc. for $C_{18}H_{14}FNO_2$: 295.1009; found: 295.1000.

*4.2.3.6. 4-(3-Fluorobenzyl)-4H-furo[3,2-b]indole-2-methanol (**7e**).* Yield: 55%; brown oil; IR (KBr) ν (cm^{-1}): 2924 (CH), 3415 (OH); ^1H NMR (500 MHz, DMSO-d_6) δ (ppm): 4.54 (d, J = 3.5 Hz, 2H), 5.40 (t, J = 3.0 Hz, 1H), 5.52 (s, 2H), 6.71 (s, 1H), 7.04–7.38 (m, 6H), 7.63 (d, J = 9.5 Hz, 1H), 7.65 (d, J = 10.5 Hz, 1H); ^{13}C NMR (125 MHz, DMSO-d_6) δ (ppm): 47.63, 57.28, 97.29, 111.29, 113.99, 114.48 (d, J = 21.25 Hz), 114.74 (d, J = 21.25 Hz), 115.94, 119.78, 121.53, 123.73 (d, J = 2.5 Hz), 131.11 (d, J = 7.5 Hz), 133.26, 139.35, 139.71, 141.27 (d, J = 7.5 Hz), 159.94, 162.65 (d, J = 242.5 Hz); MS (EI, 70 eV) m/z: 295.2 (M^+); HRMS (EI) m/z: calc. for $C_{18}H_{14}FNO_2$: 295.1009; found: 295.1011.

*4.2.3.7. 4-(4-Fluorobenzyl)-4H-furo[3,2-b]indole-2-methanol (**7f**).* Yield: 44%; white flocculence crystals; mp: 97–99 °C; IR (KBr) ν (cm^{-1}): 2933 (CH), 3213 (OH); ^1H NMR (400 MHz, DMSO-d_6) δ (ppm): 4.53 (d, J = 5.6 Hz, 2H), 5.37 (t, J = 5.6 Hz, 1H), 5.46 (s, 2H), 6.65 (s, 1H), 7.08–7.31 (m, 6H), 7.62 (d, J = 8.0 Hz, 2H); ^{13}C NMR (50 MHz, DMSO-d_6) δ (ppm): 47.42, 57.20, 97.31, 111.24, 113.89, 115.80 (d, J = 21 Hz), 115.88, 116.01, 119.69, 121.48, 129.82 (d, J = 8 Hz), 133.10, 134.43, 139.23, 139.66, 159.72; MS (EI, 70 eV) m/z: 295.2 (M^+); HRMS (EI) m/z: calc. for $C_{18}H_{14}FNO_2$: 295.1009; found: 295.1002.

*4.2.3.8. 4-(2-Chlorobenzyl)-4H-furo[3,2-b]indole-2-methanol (**7g**).* Yield: 61%; brown oil; IR (KBr) ν (cm^{-1}): 2924 (CH), 3441 (OH); ^1H NMR (400 MHz, DMSO-d_6) δ (ppm): 4.50 (d, J = 5.6 Hz, 2H), 5.35 (t, J = 5.6 Hz, 1H), 5.56 (s, 2H), 6.44 (s, 1H), 6.88 (d, J = 7.2 Hz, 1H), 7.10–7.18 (m, 2H), 7.25 (t, J = 7.2 Hz, 1H), 7.34 (td, J = 7.6, 1.2 Hz, 1H), 7.53 (dd, J = 5.2, 2.4 Hz, 2H), 7.66 (d, J = 7.2 Hz, 1H); ^{13}C NMR (50 MHz, DMSO-d_6) δ (ppm): 46.26, 57.19, 97.29, 111.19, 113.91, 115.93, 119.80, 121.55, 127.95, 129.54, 129.92, 130.01, 132.72, 133.15, 135.19, 139.46, 139.71, 159.78; MS (EI, 70 eV) m/z: 311.1 (M^+); HRMS (EI) m/z: calc. for $C_{18}H_{14}ClNO_2$: 311.0713; found: 311.0710.

*4.2.3.9. 4-(3-Chlorobenzyl)-4H-furo[3,2-b]indole-2-methanol (**7h**).* Yield: 58%; brown oil; IR (KBr) ν (cm^{-1}): 2924 (CH), 3446 (OH); ^1H NMR (400 MHz, DMSO-d_6) δ (ppm): 4.53 (d, J = 5.6 Hz, 2H), 5.38 (t, J = 5.6 Hz, 1H), 5.50 (s, 2H), 6.70 (s, 1H), 7.09–7.34 (m, 6H), 7.62 (d, J = 8.8 Hz, 1H), 7.64 (d, J = 8.8 Hz, 1H); ^{13}C NMR (50 MHz, DMSO-d_6) δ (ppm): 47.49, 57.24, 97.24, 111.26, 113.95, 115.93, 119.77, 121.52, 126.31, 127.45, 127.88, 130.98, 133.20, 133.61, 139.28, 139.66, 140.91, 159.92; MS (EI, 70 eV) m/z: 311.1 (M^+); HRMS (EI) m/z: calc. for $C_{18}H_{14}ClNO_2$: 311.0713; found: 311.0718.

*4.2.3.10. 4-(4-Chlorobenzyl)-4H-furo[3,2-b]indole-2-methanol (**7i**).* Yield: 64%; brown oil; IR (KBr) ν (cm^{-1}): 2924 (CH), 3417 (OH); ^1H NMR (400 MHz, DMSO-d_6) δ (ppm): 4.52 (d, J = 5.6 Hz, 2H), 5.36 (t, J = 5.6 Hz, 1H), 5.48 (s, 2H), 6.66 (s, 1H), 7.10 (t, J = 7.2 Hz, 1H), 7.15 (t, J = 8.0 Hz, 1H), 7.24 (d, J = 8.0 Hz, 2H), 7.37 (d, J = 8.4 Hz, 2H), 7.60 (d, J = 8.0 Hz, 1H), 7.63 (d, J = 7.6 Hz, 1H); ^{13}C NMR (50 MHz, DMSO-d_6) δ (ppm): 47.42, 57.23, 97.27, 111.27, 113.94, 115.90, 119.71, 121.46, 129.02, 129.56, 132.50, 133.18, 137.35, 139.27, 139.66, 159.86; MS (EI, 70 eV) m/z: 311.1 (M^+); HRMS (EI) m/z: calc. for $C_{18}H_{14}ClNO_2$: 311.0713; found: 311.0707.

*4.2.3.11. 4-(2-Methoxybenzyl)-4H-furo[3,2-b]indole-2-methanol (**7j**).* Yield: 60%; brown oil; IR (KBr) ν (cm^{-1}): 2924, 2954 (CH), 3427 (OH); ^1H NMR (400 MHz, DMSO-d_6) δ (ppm): 3.83 (s, 3H), 4.51 (d, J = 5.6 Hz, 2H), 5.34 (t, J = 5.6 Hz, 1H), 5.39 (s, 2H), 6.51 (s, 1H), 6.84 (t, J = 7.6 Hz, 1H), 6.91 (d, J = 6.4 Hz, 1H), 7.04 (d, J = 8.4 Hz, 1H), 7.09 (t, J = 7.2 Hz, 1H), 7.14 (t, J = 7.2 Hz, 1H), 7.27 (td, J = 1.6 and 8.0 Hz, 1H), 7.55 (d, J = 8.4 Hz, 1H), 7.62 (d, J = 7.2 Hz, 1H); ^{13}C NMR (50 MHz, DMSO-d_6) δ (ppm): 43.58, 55.83, 57.21, 97.47, 111.26, 111.36, 113.71, 115.76, 119.43, 120.73, 121.26, 125.58, 129.02, 129.50, 133.42, 139.36, 157.33, 159.59; MS (EI, 70 eV) m/z: 307.2 (M^+); HRMS (EI) m/z: calc. for $C_{19}H_{17}NO_3$: 307.1208; found: 307.1200.

*4.2.3.12. 4-(3-Methoxybenzyl)-4H-furo[3,2-b]indole-2-methanol (**7k**).* Yield: 79%; yellow oil; IR (KBr) ν (cm^{-1}): 2924, 2954 (CH), 3448 (OH); ^1H NMR (400 MHz, DMSO-d_6) δ (ppm): 3.69 (*s*, 3H), 4.52 (d, J = 5.2 Hz, 2H), 5.35 (t, J = 5.6 Hz, 1H), 5.43 (s, 2H), 6.65 (s, 1H), 6.76 (d, J = 7.6 Hz, 1H), 6.82–6.83 (m, 2H), 7.09 (t, J = 7.6 Hz, 1H), 7.15 (t, J = 7.2 Hz, 1H), 7.21 (t, J = 8.4 Hz, 1H), 7.60 (d, J = 8.0 Hz, 1H), 7.62 (d, J = 8.0 Hz, 1H); ^{13}C NMR (50 MHz, DMSO-d_6) δ (ppm): 48.10, 55.43, 57.24, 97.33, 111.31, 112.15, 112.81, 113.86, 115.85, 119.60, 119.82, 121.38, 130.15, 133.32, 139.36, 139.59, 139.86, 159.79; MS (EI, 70 eV) m/z: 307.0 (M^+); HRMS (EI) m/z: calc. for $C_{19}H_{17}NO_3$: 307.1208; found: 311.1205.

*4.2.3.13. 4-(4-Methoxybenzyl)-4H-furo[3,2-b]indole-2-methanol (**7l**).* Yield: 17%; orange cubic crystals; mp: 95–96 °C; IR (KBr) ν (cm^{-1}): 3491 (OH); ^1H NMR (400 MHz, DMSO-d_6) δ (ppm): 3.70 (s, 3H), 4.52 (d, J = 4.8 Hz, 2H), 5.34–5.38 (m, 3H), 6.60 (s, 1H), 6.86 (d, J = 8.4 Hz, 2H), 7.08 (t, J = 7.6 Hz, 1H), 7.15 (t, J = 7.6 Hz, 1H), 7.21 (d, J = 8.4 Hz, 2H), 7.61 (d, J = 6.8 Hz, 1H), 7.63 (d, J = 7.6 Hz, 1H); ^{13}C NMR (50 MHz, DMSO-d_6) δ (ppm): 47.71, 55.49, 57.24, 97.38, 111.33, 113.85, 114.38, 115.82, 119.49, 121.30, 129.30, 130.14, 133.15, 139.24, 139.59, 159.09, 159.70; MS (EI, 70 eV) m/z: 307.1 (M^+); HRMS (EI) m/z: calc. for $C_{19}H_{17}NO_3$: 307.1208; found: 307.1201.

*4.2.3.14. 4-(3,4-(Methylenedioxy)benzyl)-4H-furo[3,2-b]indole-2-methanol (**7m**).* Yield: 62%; brown oil; IR (KBr) ν (cm^{-1}): 2924 (CH),

3441 (OH); ^{1}H NMR (400 MHz, DMSO-d_6) δ (ppm): 4.53 (d, J = 5.6 Hz, 2H), 5.34–5.37 (m, 3H), 5.96 (s, 2H), 6.66 (s, 1H), 6.78 (d, J = 8.0 Hz, 1H), 6.83 (s, 1H), 6.84 (d, J = 8.4 Hz, 1H), 7.09 (t, J = 7.6 Hz, 1H), 7.16 (t, J = 7.6 Hz, 1H), 7.62 (d, J = 7.6 Hz, 1H), 7.64 (d, J = 8.4 Hz, 1H); ^{13}C NMR (50 MHz, DMSO-d_6) δ (ppm): 47.98, 57.23, 97.39, 101.43, 108.43, 108.70, 111.35, 113.87, 115.83, 119.56, 121.34, 132.01, 133.11, 139.21, 139.60, 147.04, 147.79, 159.75; MS (EI, 70 eV) m/z: 321.0 (M^+); HRMS (EI) m/z: calc. for $C_{19}H_{15}NO_4$: 321.1001; found: 321.1005.

*4.2.3.15. 4-(3-(Hydroxymethyl)benzyl)-4H-furo[3,2-b]indole-2-methanol (**7n**).* Yield: 42%; orange cubic crystals; mp: 92–94 °C; IR (KBr) ν (cm^{-1}): 2918 (CH), 3277 (OH); ^{1}H NMR (400 MHz, DMSO-d_6) δ (ppm): 4.43 (d, J = 5.6 Hz, 2H), 4.52 (d, J = 5.6 Hz, 2H), 5.15 (t, J = 5.6 Hz, 1H), 5.36 (t, J = 5.6 Hz, 1H), 5.46 (s, 2H), 6.62 (s, 1H), 7.08–7.28 (m, 6H), 7.59 (d, J = 8.0 Hz, 1H), 7.63 (d, J = 7.6 Hz, 1H); ^{13}C NMR (50 MHz, DMSO-d_6) δ (ppm): 48.29, 57.23, 63.12, 97.34, 111.27, 113.81, 115.84, 119.55, 121.37, 125.75, 126.06, 126.13, 128.76, 133.29, 138.10, 139.31, 139.55, 143.37, 159.71; MS (EI, 70 eV) m/z: 307.1 (M^+); HRMS (EI) m/z: calc. for $C_{19}H_{17}NO_3$: 307.1208; found: 307.1216.

*4.2.3.16. 4-(4-(Hydroxymethyl)benzyl)-4H-furo[3,2-b]indole-2-methanol (**7o**).* Yield: 47%; pale red flocculence crystals; mp: 140–141 °C; IR (KBr) ν (cm^{-1}): 2933 (CH), 3275 (OH); ^{1}H NMR (400 MHz, DMSO-d_6) δ (ppm): 4.44 (d, J = 5.6 Hz, 2H), 4.52 (d, J = 5.6 Hz, 2H), 5.11 (t, J = 5.6 Hz, 1H), 5.36 (t, J = 5.6 Hz, 1H), 5.44 (s, 2H), 6.63 (s, 1H), 7.09 (t, J = 7.2 Hz, 1H), 7.15 (t, J = 7.2 Hz, 1H), 7.20 (d, J = 8.0 Hz, 2H), 7.24 (d, J = 8.0 Hz, 2H), 7.61 (d, J = 5.2 Hz, 1H), 7.62 (d, J = 4.4 Hz, 1H); ^{13}C NMR (50 MHz, DMSO-d_6) δ (ppm): 48.06, 57.24, 63.05, 97.38, 111.33, 113.86, 115.85, 119.55, 121.35, 127.13, 127.63, 133.24, 136.57, 139.30, 139.59, 142.27, 159.73; MS (EI, 70 eV) m/z: 307.1 (M^+); HRMS (EI) m/z: calc. for $C_{19}H_{17}NO_3$: 307.1208; found: 307.1201.

*4.2.3.17. (5-((2-(Hydroxymethyl)-4H-furo[3,2-b]indol-4-yl)methyl) furan-2-yl) methanol (**10a**).* Yield: 60%; pale yellow cubic crystals; mp: 121–123 °C; IR (KBr) ν (cm^{-1}): 2918, 3188 (CH), 3294 (OH); ^{1}H NMR (600 MHz, DMSO-d_6) δ (ppm): 4.29 (d, J = 4.8 Hz, 2H), 4.53 (d, J = 4.8 Hz, 2H), 5.15 (t, J = 5.4 Hz, 1H), 5.38 (t, J = 5.4 Hz, 1H), 5.42 (s, 2H), 6.22 (d, J = 3.6 Hz, 1H), 6.42 (d, J = 3.0 Hz, 1H), 6.60 (s, 1H), 7.10 (t, J = 7.8 Hz, 1H), 7.17 (t, J = 8.4 Hz, 1H), 7.62 (d, J = 7.8 Hz, 1H), 7.67 (d, J = 8.4 Hz, 1H); ^{13}C NMR (150 MHz, DMSO-d_6) δ (ppm): 41.05, 55.59, 56.78, 96.90, 107.72, 109.41, 110.79, 113.43, 115.35, 119.20, 120.90, 132.54, 138.74, 139.14, 149.64, 155.53, 159.23; MS (EI, 70 eV) m/z: 297.1 (M^+); HRMS (EI) m/z: calc. for $C_{17}H_{15}NO_4$: 297.1001; found: 297.1007.

*4.2.3.18. (5-((2-(Hydroxymethyl)-4H-furo[3,2-b]indol-4-yl)methyl) thiophen-2-yl)methanol (**10b**).* Yield: 37%; pale brown flocculence crystals; mp: 143–145 °C; IR (KBr) ν (cm^{-1}): 3190 (CH), 3288 (OH); ^{1}H NMR (400 MHz, DMSO-d_6) δ (ppm): 4.49 (d, J = 5.6 Hz, 2H), 4.54 (d, J = 6.0 Hz, 2H), 5.33 (t, J = 5.6 Hz, 1H), 5.39 (t, J = 6.0 Hz, 1H), 5.61 (s, 2H), 6.72 (s, 1H), 6.76 (d, J = 3.6 Hz, 1H), 7.00 (d, J = 3.6 Hz, 1H), 7.10 (t, J = 7.6 Hz, 1H), 7.18 (t, J = 7.6 Hz, 1H), 7.61 (d, J = 8.0 Hz, 1H), 7.68 (d, J = 8.4 Hz, 1H); ^{13}C NMR (50 MHz, DMSO-d_6) δ (ppm): 43.32, 57.23, 58.74, 97.41, 111.35, 114.11, 115.86, 119.76, 121.41, 123.91, 126.46, 132.89, 139.09, 139.39, 139.82, 146.71, 159.70; MS (EI, 70 eV) m/z: 313.1 (M^+); HRMS (EI) m/z: calc. for $C_{17}H_{15}NO_3S$: 313.0773; found: 313.0778.

*4.2.3.19. (5-((2-(Hydroxymethyl)-4H-furo[3,2-b]indol-4-yl)methyl) selenophen-2-yl)methanol (**10c**).* Yield: 55%; pale yellow flocculence crystals; mp: 153–154 °C; IR (KBr) ν (cm^{-1}): 3190 (CH), 3286 (OH); ^{1}H NMR (400 MHz, DMSO-d_6) δ (ppm): 4.50 (d, J = 5.6 Hz, 2H), 4.54 (d, J = 6.0 Hz, 2H), 5.38 (t, J = 5.6 Hz, 1H), 5.42 (t, J = 5.6 Hz, 1H), 5.63 (s, 2H), 6.71 (s, 1H), 6.88 (d, J = 3.6 Hz, 1H), 7.08–7.19 (m, 3H), 7.61 (d, J = 7.6 Hz, 1H), 7.66 (d, J = 8.0 Hz, 1H); ^{13}C NMR (50 MHz, DMSO-d_6) δ (ppm): 45.69, 57.23, 60.89, 97.43, 111.38, 114.20, 115.87, 119.76, 121.37, 124.65, 128.40, 132.88, 139.13, 139.90, 145.70, 154.85, 159.74; MS (EI, 70 eV) m/z: 361.1 (M^+); HRMS (EI) m/z: calc. for $C_{17}H_{15}NO_3Se$: 361.0217; found: 361.0214.

4.3. Biological evaluation

4.3.1. Cell culture and treatment

Human cancer cell lines were purchased from ATCC (Manassas, VA) or the BCRC. Human leukemia HL-60, non-small-cell-lung cancer H460, and COLO 205 cancer cells were maintained in an RPMI-1640 medium supplemented with 10% fetal bovine serum (FBS) (GIBCO/BRL), penicillin (100 U/mL)/streptomycin (100 g/mL) (GIBCO/BRL) and 1% L-glutamine (GIBCO/BRL) at 37 °C in a humidified atmosphere containing 5% CO_2. Human hepatoma Hep 3B and human fetal skin fibroblasts Detroit 551 cells were maintained in a DMEM supplemented with 10% FBS, penicillin (100 U/mL)/streptomycin (100 g/mL) and 1% L-glutamine at 37 °C in a humidified atmosphere containing 5% CO_2. Logarithmically growing cancer cells were used for all experiments. The A498 renal cancer cells were maintained in an MEM supplemented with 10% FBS, penicillin (100 U/mL)/streptomycin (100 g/mL), and 1% L-glutamine at 37 °C in a humidified atmosphere containing 5% CO_2.

4.3.2. Cytotoxicity assay

Cytotoxicity was assessed using a 3-(4,5-dimethylthiazol-2-yl)-2,5- diphenyltetrazolium bromide (MTT) assay [16]. HL-60, Hep 3B, H460 and Detroit 551 cells were treated with vehicle or test compounds for 48 h. After treatment, the cells were washed once with PBS and incubated with 50 μL MTT for 2 h. The formazan precipitate was then dissolved in 150 μL DMSO, and the absorbance was measured on an ELISA reader at a wavelength of 570 nm.

4.3.3. Cell morphology

The A498 cells were plated at a density of 5 × 10^5 cells per well in a 10 cm dish and then incubated with 0.5 μM of **10a** for 12–48 h. Cells were directly examined and photographed under a phase contrast microscope.

4.3.4. Quantification of apoptosis

The A498 cells (5 × 10^5 cells/dish) were fluorescently labeled for detecting apoptotic and necrotic cells by adding 100 μL of a binding buffer, 2 μL of annexin V-FITC, and 2 μL of PI to each sample. The samples were mixed gently and incubated at room temperature in the dark for 15 min. In total, 300 μL of the binding buffer was immediately added-to each sample before flow cytometric analysis. A minimum of 10 000 cells within the gated region were analyzed. The Annexin V-FITC Apoptosis Detection Kit was obtained from Strong Biotech Corporation (Strong Biotech, Taiwan).

4.3.5. Flow cytometric analysis for cell-cycle effects [17]

Cells were fixed in 70% ethanol overnight and re-suspended in PBS containing 20 μg/mL PI (Sigma Chemical Co., St. Louis, MO, USA), 0.2 mg/mL RNase A (Sigma Chemical Co., St. Louis, MO, USA), and 0.1% Triton X-100 (Sigma Chemical Co., St. Louis, MO, USA) in a dark room. Following 30 min of incubation at 37 °C, cell-cycle distribution was analyzed using ModFit LT software (Verity Software House, Topsham, USA) in a BD FACSCanto flow cytometer (Becton Dickinson, San Jose, CA).

4.3.6. Mitochondrial membrane potential analysis

Cells were plated in 6-well plates at 5.0 × 10^5 cells/dish and treated with 0.5 μM **10a** for 6–48 h. Mitochondrial membranes were stained by adding 0.5 mL of a JC-1 working solution (JC-1 according to the protocol on a BD™ MitoScreen as described in the section Methods for Staining Cells with JC-1 and Analyzing by Flow Cytometry) to each sample. Samples were incubated for 10–15 min

at 37 °C in the dark. The mitochondrial membrane potential was measured using the BD FACSCanto flow cytometer (Becton Dickinson, San Jose, CA).

4.3.7. Western blot assay

Treated cells were collected and washed with PBS. After centrifugation, cells were lysed in a lysis buffer. The lysates were incubated on ice for 30 min and centrifuged at 12 000*g* for 20 min. Supernatants were collected, and protein concentrations were then determined using the Bradford Assay. After adding a 5× sample loading buffer containing 625 mM Tris–HCl (Sigma Chemical Co. St. Louis, MO, USA), pH = 6.8, 500 mM dithiothreitol (BIO-RAD), 10% SDS (BIO-RAD), 0.06% bromophenol blue (Merck), and 50% glycerol (AMRESCO), the protein samples were electrophoresed on 10% SDS-polyacrylamide gels and transferred to a nitrocellulose membrane (Amersham Pharmacia Biotech, Piscataway, NJ, USA). Immunoreactivity was detected using the western blot chemiluminescence reagent system (PerkinElmer Life Sciences, Inc., Boston, MA). β-Actin (Chemicon International, Inc., Temecula, CA, USA) was used as a loading control.

4.3.8. Statistical analysis

Statistical analysis was performed using analysis of variance (ANOVA) followed by Turkey's test. All data were expressed as the mean ± SD from at least three independent experiments. $^{*}P < 0.001$ was indicative of a statistically significant difference.

4.3.9. In vivo antitumor activity assay

Male BALB/cAnN.Cg-Foxn1nu/CrlNarl nude mice (18–20 g; 4–6 weeks of age) were purchased from the National Animal Center and maintained in pressurized ventilated cages according to institutional regulations. Nude mice were subcutaneously inoculated with A498 cells at 2×10^6 cells per mouse in 0.1 mL PBS by using a 24G needle. After the appearance of a 100 mm^3 tumor nodule, tumor-bearing mice were randomly assigned to several groups (eight animals in each group). The mice were administered a single ip dose 5 times per week for 4 consecutive weeks at 30 mg/kg or 60 mg/kg. Body weight and tumor size were measured and recorded every 7 days during the experiment period of 28 days. Tumor volume was calculated using the following formula: $1/2\ (L + W^2)$, where L is the length and W is the width [18,19]. At the end of the experiments, the animals were euthanized with carbon dioxide before cervical dislocation. The tumors were excised, weighed, and sectioned, and the tumor sections were embedded in an OCT compound and frozen at −70 °C.

Acknowledgments

This investigation was supported by research grants from the National Science Council of the Republic of China awarded to L.J. Huang (NSC 98-2628-B-039-018-MY3; NSC 101-2320-B-039-009-MY3). Experiments and data analysis were partially performed using the Medical Research Core Facilities Center, Office of Research & Development, China Medical University, Taichung, Taiwan, ROC.

Appendix A. Supplementary data

Supplementary data related to this article can be found at http://dx.doi.org/10.1016/j.ejmech.2013.06.012.

References

[1] H.K. Hsu, S.H. Juan, P.Y. Ho, Y.C. Liang, C.H. Lin, C.M. Teng, W.S. Lee, YC-1 inhibits proliferation of human vascular endothelial cells through a cyclic GMP-independent pathway, Biochem. Pharmacol. 66 (2003) 263–271.
[2] S.L. Pan, J.H. Guh, C.Y. Peng, S.W. Wang, Y.L. Chang, F.C. Cheng, J.H. Chang, S.C. Kuo, F.Y. Lee, C.M. Teng, YC-1 [3-(5′-Hydroxymethyl-2′-furyl) -1-benzyl indazole] inhibits endothelial cell functions induced by angiogenic factors in vitro and angiogenesis in vivo models, J. Pharmacol. Exp. Ther. 314 (2005) 35–42.
[3] S.L. Pan, J.H. Guh, C.Y. Peng, Y.L. Chang, F.C. Cheng, J.H. Chang, S.C. Kuo, F.Y. Lee, C.M. Teng, A potential role of YC-1 on the inhibition of cytokine release in peripheral blood mononuclear leukocytes and endotoxemic mouse models, Thromb. Haemost. 93 (2005) 940–948.
[4] S.W. Wang, S.L. Pan, J.H. Guh, H.L. Chen, D.M. Huang, Y.L. Chang, S.C. Kuo, F.Y. Lee, C.M. Teng, YC-1 [3-(5′-Hydroxymethyl-2′-furyl)-1-benzyl indazole] exhibits a novel antiproliferative effect and arrests the cell cycle in G0-G1 in human hepatocellular carcinoma cells, J. Pharmacol. Exp. Ther. 312 (2005) 917–925.
[5] Y.T. Huang, S.L. Pan, J.H. Guh, Y.L. Chang, F.Y. Lee, S.C. Kuo, C.M. Teng, YC-1 suppresses constitutive nuclear factor-κB activation and induces apoptosis in human prostate cancer cells, Mol. Cancer Ther. 4 (2005) 1628–1635.
[6] Y.N. Liu, S.L. Pan, C.Y. Peng, J.H. Guh, D.M. Huang, Y.L. Chang, C.H. Lin, H.C. Pai, S.C. Kuo, F.Y. Lee, C.M. Teng, YC-1 [3-(5′-Hydroxymethyl-2′-furyl)-1-benzyl indazole] inhibits neointima formation in balloon-injured rat carotid through suppression of expressions and activities of matrix metalloproteinases 2 and 9, J. Pharmacol. Exp. Ther. 316 (2006) 35–41.
[7] S.Y. Wu, S.L. Pan, T.H. Chen, C.H. Liao, D.Y. Huang, J.H. Guh, Y.L. Chang, S.C. Kuo, F.Y. Lee, C.M. Teng, YC-1 induces apoptosis of human renal carcinoma A498 cells *in vitro* and *in vivo* through activation of the JNK pathway, Br. J. Pharmacol. 155 (2008) 505–513.
[8] Y. Cheng, W. Li, Y. Liu, H.C. Cheng, J. Ma, L. Qiu, YC-1 exerts inhibitory effects on MDA-MB-468 breast cancer cells by targeting EGFR *in vitro* and *in vivo* under normoxic condition, Chin. J. Cancer 31 (2012) 248–256.
[9] L.C. Chou, L.J. Huang, J.S. Yang, F.Y. Lee, C.M. Tengc, S.C. Kuo, Synthesis of furopyrazole analogs of 1-benzyl-3-(5-hydroxymethyl-2-furyl)indazole (YC-1) as novel anti-leukemia agents, Bioorg. Med. Chem. 15 (2007) 1732–1740.
[10] S.C. Kuo, F.Y. Lee, C.M. Teng, 1-(Substituted benzyl)-3-(substituted aryl)-condensed pyrazole derivatives and processed of making the same, U.S. Patent 5574168, 1996.
[11] L.C. Chou, L.J. Huang, M.H. Hsu, M.C. Fang, J.S. Yang, S.H. Zhuang, H.Y. Lin, F.Y. Lee, C.M. Teng, S.C. Kuo, Synthesis of 1-benzyl-3-(5-hydroxymethyl-2-furyl)selenolo[3,2-*c*]pyrazole derivatives as new anticancer agents, Eur. J. Med. Chem. 45 (2010) 1395–1402.
[12] Y. Nakashima, Y. Kawashima, F. Amanuma, K. Sota, A. Tanaka, T. Kameyama, Furo [3, 2-*b*] indole derivatives. I. Synthesis and analgesic and anti-inflammatory activities of 4, 6-disubstituted-furo [3,2-*b*] indole-2-carboxamide derivatives, Chem. Pharm. Bull. 32 (1984) 4271–4280.
[13] S. Tsuboi, S. Minura, S.I. Ono, K. Watanabe, A. Takeda, Oxidation of 2,4-alkadienoic esters with selenium dioxide. A new synthesis of furan and selenophenes, Bull. Chem. Soc. Jpn. 60 (1987) 1807–1812.
[14] A. Monks, D. Scudiero, P. Skehan, R. Shoemaker, K. Paull, D. Vistica, C. Hose, J. Langley, P. Cronise, A. Vaigro-Wolff, M. Gray-Goodrich, H. Campbell, J. Mayo, M. Boyd, Feasibility of a high-flux anticancer drug screen using a diverse panel of cultured human tumor cell lines, J. Natl. Cancer Inst. 83 (1991) 757–766.
[15] C.J. Chen, M.H. Hsu, L.J. Huang, T. Yamori, J.G. Chung, F.Y. Lee, C.M. Teng, S.C. Kuo, Anticancer mechanisms of YC-1 in human lung cancer cell line, NCI-H226, Biochem. Pharmacol. 75 (2008) 360–368.
[16] M.V. Berridge, A.S. Tan, Characterization of the cellular reduction of 3-(4,5-dimethylthiazol-2-yl)-2,5-diphenyltetrazolium bromide (MTT): subcellular localization, substrate dependence, and involvement of mitochondrial electron transport in MTT reduction, Arch. Biochem. Biophys. 303 (1993) 474–482.
[17] P.E. Newburger, C. Speier, N. Borregaard, C.E. Walsh, J.C. Whitin, E.R. Simons, Development of the superoxide-generating system during differentiation of the HL-60 human promyelocytic leukemia cell line, J. Biol. Chem. 259 (1984) 3771–3776.
[18] D.M. Euhus, C. Hudd, M.C. LaRegina, F.E. Johnson, Tumor measurement in the nude mouse, J. Surg. Oncol. 31 (1986) 229–234.
[19] M.M. Tomayko, C.P. Reynolds, Determination of subcutaneous tumor size in athymic (nude) mice, Cancer Chemother. Pharmacol. 24 (1989) 148–154.
[20] G.P. Margison, M.F.S. Koref, A.C. Povey, Mechanisms of carcinogenicity/chemotherapy by O^6-methylguanine, Mutagenesis 17 (2002) 483–487.
[21] S. Lakhanpal, R.C. Donehower, E.K. Rowinsky, Phase II study of 4-Ipomeanol, a naturally occurring alkylating furan, in patients with advanced hepatocellular carcinoma, Invest. New Drugs 19 (2001) 69–76.
[22] M. Cuendet, K. Christov, D.D. Lantvit, Y. Deng, S. Hedayat, L. Helson, J.D. McChesney, J.M. Pezzuto, Multiple myeloma regression mediated by bruceantin, Clin. Cancer Res. 10 (2004) 1170–1179.
[23] S.R. Patel, L.K. Kvols, J. Rubin, M.J. O'Connell, J.H. Edmonson, M.M. Ames, J.S. Kovach, Phase I–II study of pibenzimol hydrochloride (NSC 322921) in advanced pancreatic carcinoma, Invest. New Drugs 9 (1991) 53–57.
[24] G. Northrop, S.G. Taylor III, R.I. Northrop, Biochemical effects of mithramycin on cultured cells, Cancer Res. 29 (1969) 1916–1919.

[25] C.R. Garrett, D. Coppola, R.M. Wenham, C.L. Cubitt, A.M. Neuger, T.J. Frost, R.M. Lush, D.M. Sullivan, J.Q. Cheng, S.M. Sebti, Phase I pharmacokinetic and pharmacodynamic study of triciribine phosphate monohydrate, a small-molecule inhibitor of AKT phosphorylation, in adult subjects with solid tumors containing activated AKT, Invest. New Drugs 29 (2011) 1381–1389.
[26] J. Westendorf, M. Aydin, G. Groth, O. Weller, H. Marquardt, Mechanistic aspects of DNA damage by morpholinyl and cyanomorpholinyl anthracyclines, Cancer Res. 49 (1989) 5262–5266.
[27] J.L. Nitiss, P. Pourquier, Y. Pommier, Aclacinomycin A stabilizes topoisomerase I covalent complexes, Cancer Res. 57 (1997) 4564–4569.
[28] H. Gao, E.F. Yamasaki, K.K. Chan, L.L. Shen, R.M. Snapka, Chloroquinoxaline sulfonamide (NSC 339004) is a topoisomerase IIa/b poison, Cancer Res. 60 (2000) 5937–5940.
[29] L.G. May, M.A. Madine, M.J. Waring, Echinomycin inhibits chromosomal DNA replication and embryonic development in vertebrates, Nucleic Acids Res. 32 (2004) 65–72.